Calhoun: The NPS Institutional Archive

DSpace Repository

Theses and Dissertations | 1. Thesis and Dissertation Collection, all items

1994

Construction and wind tunnel test of a 1/12th scale helicopter model

Capasso, Michael Anthony

Monterey, California. Naval Postgraduate School

http://hdl.handle.net/10945/30925

This publication is a work of the U.S. Government as defined in Title 17, United States Code, Section 101. Copyright protection is not available for this work in the United States.

Downloaded from NPS Archive: Calhoun

http://www.nps.edu/library

Calhoun is the Naval Postgraduate School's public access digital repository for research materials and institutional publications created by the NPS community. Calhoun is named for Professor of Mathematics Guy K. Calhoun, NPS's first appointed -- and published -- scholarly author.

Dudley Knox Library / Naval Postgraduate School
411 Dyer Road / 1 University Circle
Monterey, California USA 93943

NAVAL POSTGRADUATE SCHOOL
MONTEREY, CALIFORNIA

THESIS

CONSTRUCTION AND WIND TUNNEL TEST OF A 1/12th SCALE HELICOPTER MODEL

by

Michael Anthony Capasso

September, 1994

Thesis Advisor: E. Roberts Wood

Approved for public release; distribution is unlimited.

Thesis
C19475

DUDLEY KNOX LIBRARY
NAVAL POSTGRADUATE SCHOOL
MONTEREY CA 93943-5101

REPORT DOCUMENTATION PAGE

Form Approved OMB No. 0704-0188

Public reporting burden for this collection of information is estimated to average 1 hour per response, including the time for reviewing instruction, searching existing data sources, gathering and maintaining the data needed, and completing and reviewing the collection of information. Send comments regarding this burden estimate or any other aspect of this collection of information, including suggestions for reducing this burden, to Washington Headquarters Services, Directorate for Information Operations and Reports, 1215 Jefferson Davis Highway, Suite 1204, Arlington, VA 22202-4302, and to the Office of Management and Budget, Paperwork Reduction Project (0704-0188) Washington DC 20503.

1. AGENCY USE ONLY *(Leave blank)*	2. REPORT DATE September 1994.	3. REPORT TYPE AND DATES COVERED Master's Thesis

4. TITLE AND SUBTITLE CONSTRUCTION AND WIND TUNNEL TEST OF A 1/12th SCALE HELICOPTER MODEL	5. FUNDING NUMBERS
6. AUTHOR(S) Capasso, Michael A.	
7. PERFORMING ORGANIZATION NAME(S) AND ADDRESS(ES) Naval Postgraduate School Monterey CA 93943-5000	8. PERFORMING ORGANIZATION REPORT NUMBER
9. SPONSORING/MONITORING AGENCY NAME(S) AND ADDRESS(ES)	10. SPONSORING/MONITORING AGENCY REPORT NUMBER

11. SUPPLEMENTARY NOTES The views expressed in this thesis are those of the author and do not reflect the official policy or position of the Department of Defense or the U.S. Government.

12a. DISTRIBUTION/AVAILABILITY STATEMENT Approved for public release; distribution is unlimited.	12b. DISTRIBUTION CODE A

13. ABSTRACT *(maximum 200 words)*

This thesis reports on the construction of a 1/12th scale model of the award winning Arapaho attack helicopter design and wind tunnel test to determine both the model and full scale equivalent flat plate area. Tests were conducted for 1g level flight and included yawed flight conditions up to 10 degrees. The significance of equivalent flat plate area for helicopters is that it is the principal parameter that establishes rotor propulsive force requirements. The Model was constructed from the original design submitted by the 1993 NPS Helicopter Design Team and is 47.5 inches long with a 48-inch main rotor diameter. The model was tested in the NPS Low Speed Wind Tunnel to measure the drag force on the main body of the model at wind tunnel velocities up to 72 knots. Drag force on the model was also measured with the rotor head and longbow radome installed, and at various yaw angles up to 10 degrees. The equivalent flat plate area was then calculated from these measurements and compared to other helicopters. Recommendations for further wind tunnel testing were made.

14. SUBJECT TERMS Low Speed Wind Tunnel, Arapaho, Helicopter Model, Equivalent Flat Plate Drag Calculation.			15. NUMBER OF PAGES 81
			16. PRICE CODE
17. SECURITY CLASSIFICATION OF REPORT Unclassified	18. SECURITY CLASSIFICATION OF THIS PAGE Unclassified	19. SECURITY CLASSIFICATION OF ABSTRACT Unclassified	20. LIMITATION OF ABSTRACT UL

NSN 7540-01-280-5500

Standard Form 298 (Rev. 2-89)
Prescribed by ANSI Std. 239-18 298-102

Approved for public release; distribution is unlimited.

CONSTRUCTION AND WIND TUNNEL TEST
OF A
1/12th SCALE HELICOPTER MODEL

by

Michael Anthony Capasso
Lieutenant Commander, United States Navy
B.S., Rutgers University, 1982

Submitted in partial fulfillment
of the requirements for the degree of

MASTER OF SCIENCE IN AERONAUTICAL ENGINEERING

from the

NAVAL POSTGRADUATE SCHOOL
September 1994

Author: [redacted]
Michael Anthony Capasso

Approved by: [redacted]
E. Roberts Wood, Thesis Advisor

[redacted]
S.K. Hebbar, Second Reader

[redacted]
Daniel J. Collins, Chairman
Department of Aeronautics and Astronautics

ABSTRACT

This thesis reports on the construction of a 1/12th scale model of the award winning Arapaho attack helicopter design and wind tunnel test to determine both the model and full scale equivalent flat plate area. Tests were conducted for 1g level flight and included yawed flight conditions up to 10 degrees. The significance of equivalent flat plate area for helicopters is that it is the principal parameter that establishes rotor propulsive force requirements. The Model was constructed from the original design submitted by the 1993 NPS Helicopter Design Team and is 47.5 inches long with a 48-inch main rotor diameter. The model was tested in the NPS Low Speed Wind Tunnel to measure the drag force on the main body of the model at wind tunnel velocities up to 72 knots. Drag force on the model was also measured with the rotor head and longbow radome installed, and at various yaw angles up to 10 degrees. The equivalent flat plate area was then calculated from these measurements and compared to other helicopters. Recommendations for further wind tunnel testing were made.

Thesis
C1947S
c.2

TABLE OF CONTENTS

I. INTRODUCTION 1
II. BACKGROUND 5
A. PROPOSAL REQUIREMENTS 5
1. Performance Requirements 5
2. Design Requirements 5
B. PRELIMINARY DESIGN SUBMISSION 7
1. Major Design Features 8
2. Arapaho Description 8
a. Fuselage 8
b. Wing Assembly 9
c. Engine and Drive System 9
d. Fuel System 9
e. Flight Controls 10
f. Main Rotor 10
g. NOTAR™ Anti-torque System 11
h. Landing Gear 11
i. Armament 11
III. CONSTRUCTION OF THE MODEL 13
A. FORWARD FUSELAGE 13
1. Nose Section 13
2. Engine Intakes and Cowlings. 15
3. Weapons Bay 17
4. Canopy 17
5. Final Shaping of the Fuselage 20
B. TAIL BOOM 20
C. WINGS 22
D. VERTICAL AND HORIZONTAL TAIL 22
E. ROTOR SYSTEM 22
1. Rotor Hub 22

DUDLEY KNOX LIBRARY
NAVAL POSTGRADUATE SCHOOL
MONTEREY CA 93943-5101

2. Rotor Blades 27
F. WEAPON SYSTEMS 27
1. Longbow Radar 28
2. Stinger Pods 28
3. Gun Turret 30
G. FINAL ASSEMBLY 30
IV. EXPERIMENTAL PROCEDURE 33
A. PREPARATION 33
1. Blockage Effects 33
2. Lift Estimation 34
3. Drag Estimation 35
4. Data Acquisition Setup 36
5. Balance Calibration 37
6. Mounting the Model 37
B. TEST RUNS 37
1. Test Section Velocity 40
a. Velocity Measurement Devices 40
b. Velocity Calculation 40
c. Velocity Corrections 41
2. Data Collection 41
a. Model Stand 42
b. Model Fuselage 42
c. Model with Rotor Hub and Longbow Radome 43
d. Model at Varying Yaw Angles 46
V. ANALYSIS 49
A. COMPARISON OF WIND TUNNEL RESULTS TO ESTIMATED DATA 49
B. COMPARISON OF VARIOUS CONFIGURATIONS 50
C. COMPARISON TO OTHER HELICOPTERS 51
VI. CONCLUSIONS AND RECOMMENDATIONS 53
APPENDIX A. 55
APPENDIX B. 59
LIST OF REFERENCES 71
INITIAL DISTRIBUTION LIST 73

ACKNOWLEDGMENTS

I wish to acknowledge the support and assistance provided by the following individuals: Professors Rick Howard and S. Hebbar for their advice and assistance, Harry Taylor of McDonnell Douglas Helicopters for the information on the Apache helicopter; Jack King for his assistance with the wind tunnel, and Alvin Lau from the Graphics Department for his fine drawings. A Very Special thanks go to Professor Bob Wood, my thesis advisor, and Ron Ramaker, without whose skill the Arapaho model could never have been built.

I. INTRODUCTION

The Arapaho design was developed by the 1993 Naval Postgraduate School (NPS) Helicopter Design Class as the Naval Postgraduate School's entry proposal in the 1993 American Helicopter Society's helicopter design competition. The objective of the design competition was to produce a preliminary design of a high speed, highly maneuverable rotorcraft, operable from unprepared surfaces to perform United States Army attack missions. The requirements of the RFP were written by McDonnell Douglas Helicopter Company and specified a range and endurance of 430 km, plus 20 minutes of combat, plus a 20 minute reserve; a speed of 200 kts.; a rate of climb of 800 ft/min.; a payload of hellfire and stinger missiles, and 30mm ammunition; a maximum load factor of 4 g's transient, and 2 g's sustained; and a ferry range of 1260 nm with a 100 nm reserve.

The Arapaho model is a 1/12th scale model based on the NPS design. The model was built primarily of wood (hard pine) with some metal and plastic parts and accessories. The structure of the model was kept as close as possible to the original design with some minor modifications due to limitations in construction capabilities and omissions in the design drawings.

The purpose of building the model was twofold: (1) to display at the 1994 American Helicopter Society's 50th Anniversary National Forum; and (2) to serve as a test model for wind tunnel tests designed to explore the drag characteristics of the unique Arapaho fuselage design. The wind tunnel testing of the scale model, the next logical step in the

design process, was to measure drag force on the model at various airspeeds so as to find equivalent flat plate area of the model and then extrapolate to full scale aircraft.

In order to analyze helicopter performance, certain basic information is required [Ref. 1, p. 273]: rotor performance, engine performance, power losses in transmissions and accessories, vertical drag in hover, tail rotor-fin interference, and parasite drag in forward flight. In this thesis, the parasite drag of the Arapaho design is determined for comparison against the drag of other helicopters. The method used to define parasite drag is to define an equivalent flat plate area of the design, a procedure commonly used in the helicopter industry. [Ref. 1, p. 132] Equivalent flat plate area is basically the frontal area of a flat plate with a drag coefficient of 1, and calculated as the drag divided by dynamic pressure:

$$f = \frac{D}{q_\infty} \tag{1.1}$$

The importance of determining the equivalent flat plate area and, in turn, the parasite drag is that it has a direct correlation to the power required to propel the helicopter through the air in forward flight. The parasite power equation [Ref. 1, p.132]

$$\text{h.p.}_p = \frac{D_p V}{550} = \frac{f \rho V^3}{1100} \tag{1.2}$$

and an approximation for the angle of attack of the helicopter's tip path plane [Ref. 1, p.133]

$$\alpha_{TPP} \cong -57.3 \frac{f}{A_b} \times \frac{\mu^2/2}{C_T/\sigma} \tag{1.3}$$

where

A_b = area of the rotor blades

C_T = Coefficient of thrust

μ = tip speed ratio

σ = solidity of rotor

can be written in terms of the equivalent flat plate area, f.

In this thesis, the objective is to describe the design and the design process, provide a detailed description of the model fabrication, document the preparation and testing of the model in the NPS wind tunnel., and estimate the equivalent flat plate area. Next, the experimental equivalent flat plate area is to be compared to a theoretically derived equivalent flat plate area. Finally, the equivalent flat plate area of the model will be scaled up to full size and compared against other helicopters whose drag values are known.

II. BACKGROUND

A. PROPOSAL REQUIREMENTS

The request for proposal (RFP) requirements were written by McDonnell Douglas Helicopter Company. [Ref. 2] The objective of the competition was to produce a preliminary design of a high speed, highly maneuverable attack helicopter which would be affordable, rugged, reliable, and easy to operate and maintain under harsh battlefield conditions.

1. Performance Requirements

The performance specified for Range and Endurance was 430 km cruise, plus 20 minutes combat (10 minutes at Intermediate Rated Power, and 10 minutes at Maximum Rated Power), plus 30 minute reserve at best endurance airspeed, plus 5 minutes at Intermediate Rated Power (IRP) for takeoff and landing. The RFP specified a level flight speed at IRP of 200 kts and a rate of climb at IRP of 800 fpm. The aircraft was required to meet these performance requirements at Primary Mission Gross Weight, at an altitude of 4000 ft., and at 95 degrees Fahrenheit.

2. Design Requirements

The design requirements specified by the RFP were to design an attack helicopter using technology that would be readily available in 1995. The helicopter must use either shaft or reaction drive with a recommendation to use production engines. A minimum of two main drive engines which use standard Army fuels was required for safety and

survivability. An onboard Auxiliary Power Unit (APU), which uses the same fuel as the main engines was required for engine starting and for maintenance activities. The APU should supply electrical, hydraulic, and/or pneumatic power as needed. Main transmission ratings, if main rotor is shaft driven, were specified as 100% of Engine Maximum Continuous Rating (Transmission Maximum Continuous Rating) at standard sea level, and 100% of Engine Maximum One Engine Inoperative (OEI) Rating at standard sea level (Transmission Emergency Rating).

The rotor system requirements specified by the RFP included a maximum main rotor disc loading of 15 lbs/ft^2, a main rotor maximum normal operating tip speed of 725 ft/sec, an anti-torque system maximum normal operating tip speed of 650 ft/sec (unless it is enclosed), and an autorotation t/k index of less than .8 seconds. An additional requirement was the capability to engage and disengage rotors safely in winds up to 60 kts.

Structural design envelope requirements for limit load factor as specified by the RFP are given by Figure 1 in Reference 2. The ultimate load factor was given as 1.5 times the limit load factor. The landing load factor was given as 2.5 g's. The Never Exceed airspeed (V_{NE}) was given as 1.2 times the level flight speed at IRP (V_H).

Weapon system requirements specified in the RFP included a 30mm turreted cannon, the ability to carry and launch a combination of Hellfire Air-to-Surface and Stinger Air-to-Air missiles along with the sensors required to deploy each system.

Other miscellaneous requirements included a two man crew, cockpit cooling system, and the ability to carry both internal and external fuel. The aircraft must be

transportable by C-141B aircraft. The aircraft was required to be crashworthy and have the same ballistic hardening and survivability as specified for the McDonnell Douglas Apache helicopter, including Infra-Red suppressor on the main engine exhausts. The design was also required to meet MIL-H-8501A Handling qualities and have minimum vibration levels.

Finally, the RFP required that the design proposals use methods of design that would ensure low cost production of the aircraft.

B. PRELIMINARY DESIGN SUBMISSION

The design proposal submitted by the 1993 NPS Helicopter Design Team was known as the Arapaho. [Ref. 3] It was a twin engine, tandem seat, single rotor attack helicopter designed to meet or exceed all competition specifications, as shown in Figure 2.1.

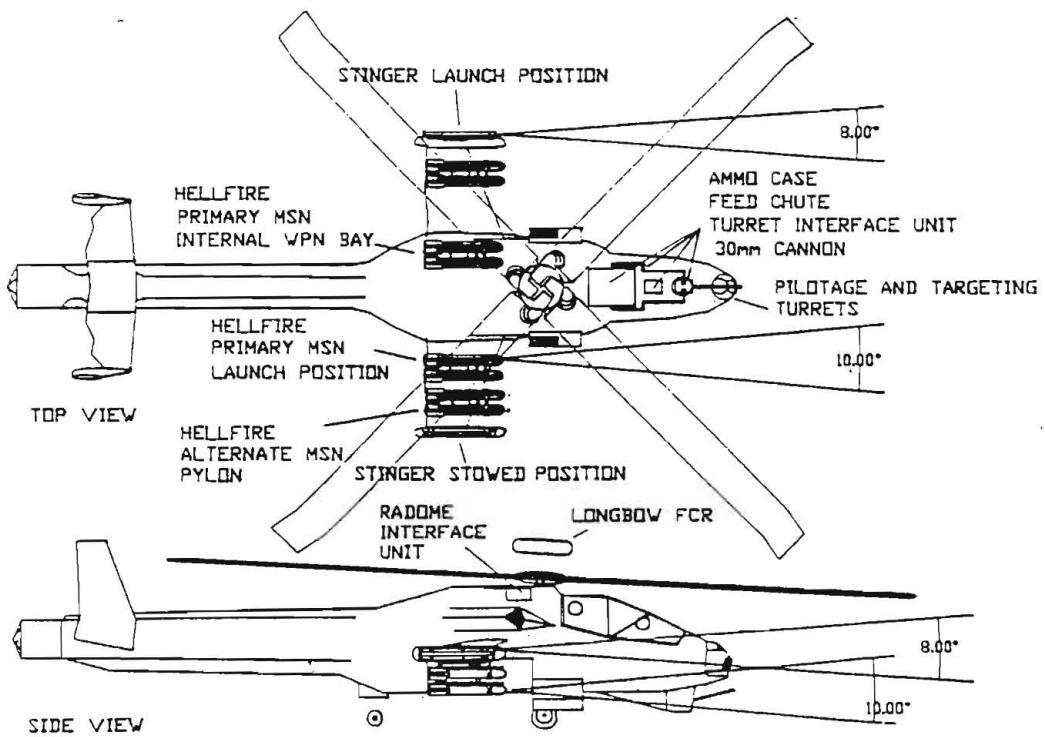

Figure 2.1 Arapaho Attack Helicopter

1. Major Design Features

The design team chose a compound helicopter design because of its ability to attain speeds of 200 kts, as well as its maneuverability, low fuel consumption, low weight, low cost, low risk technology, and high maintainability. A compound helicopter by definition is a conventional helicopter with a wing. Auxiliary propulsion may be added. The Arapaho had no auxiliary propulsion.

Other major design features included a NOTAR™ anti-torque system, movable horizontal and vertical tail, internal weapons bay, external 30mm turreted cannon, retractable landing gear, composite construction, and low observable shape. The features were selected in the conceptual phase of the design by comparing the relative merits of current helicopter design technology.

2. Arapaho Description

a. Fuselage

The fuselage was constructed primarily of composite materials supported by a primary load bearing composite keel beam to enhance overall aircraft survivability. The main part of the fuselage was designed with faceted surfaces to reduce radar cross-section. One of the objectives of the subsequent wind tunnel test program was to investigate the drag penalty introduced by these faceted surfaces. The forward section included a tandem cockpit with the 30mm cannon mounted under the nose of the aircraft. The tandem cockpit had the pilot in front for greater visibility, and the copilot/gunner in back. The engine and drive transmission systems, internal weapons bays, fuel cells, landing gear, and wings were located in the center. The tail section included the NOTAR™ antitorque

system, aft section of the integral infrared suppressor system, and horizontal and vertical tails.

b. Wing Assembly

The function of the wings of the Arapaho was to unload the rotor in high-speed flight to delay the onset of blade stall. The wings of the aircraft were designed using composite/graphite construction and provided 20% of the total lift in high-speed (180-200 knots) forward flight. The wings incorporated trailing edge flaps which automatically deploy during maneuvers exceeding 1.5g in forward flight. The outboard wing section were designed to be removable to facilitate transportation on a C-141B Starlifter aircraft. The inboard wing root section contained a portion of the upper fuel cells. Additionally the wings were designed to mount the Stinger Air-to-Air missiles on the tips, and provide hard points for additional Hellfire missiles or auxiliary fuel tanks.

c. Engine and Drive System

The helicopter was designed to be powered by two General Electric T-700 series turboshaft engines, each providing 2365 SHP, which were separated by a ballistic shield for survivability. The APU was mounted between the two main engines, as well. The main transmission was a split-torque design with power from the main engines supplied to it through nose-mounted engine gear boxes, shafts, and sprague clutches.

d. Fuel System

The fuel system was designed to provide fuel to both main engines and the APU. The design included five internal self-sealing, crash resistant fuel cells (one forward cell, two aft cells, and two wing root cells) containing a total of 311 gallons. In addition,

the aircraft was designed to carry auxiliary 383 gallon tanks in the internal weapons bays and/or 130 gallon jettisonable tanks on wing hardpoints. The design called for the capability to transfer fuel between the cells and tanks either automatically or manually, and for the engines to be fed from any cell or tank.

e. Flight Controls

The aircraft flight control system was designed using fiber optics (fly-by-light), hydraulic actuators at the rotor hub assembly, and digital automatic stabilization equipment (DASE). The NOTAR™-equipped tail boom included a direct jet thruster cylindrical assembly with its control system and movable horizontal stabilator and vertical tail surfaces. The DASE augments the stability and improves the maneuverability of the helicopter. The NOTAR™ direct jet thruster augments the coanda anti-torque force generated by the slotted tail boom and provides additional yaw control in low-speed flight, while the vertical and horizontal tail systems augment yaw and pitch control in high-speed forward flight.

f. Main Rotor

The main rotor was designed as a four-bladed, bearingless system with a 30" blade chord and a 24' radius. Each blade utilized Boeing VR-12 airfoils out to 85% radius, and a linear taper down to a VR-15 section at the tip. The blades incorporated 10 degree swept back tips and -10 degree linear blade twist. The blades were designed with four integral spars to survive a 23mm HEI round hit. The blades were mounted on a titanium hub designed for easy blade removal to enhance transportability.

g. NOTAR™ Anti-torque System

The anti-torque system was a NOTAR™ design incorporated into the tail boom. The tail boom was made from composites and incorporated the Infrared suppressor system and flight control system conduits. The coanda slots, for circulation control, were placed at the 70 and 140 degree locations relative to the downwash angle of the average rotor induced velocity vector. As previously noted, a thruster on the aft end of the tail boom provided additional yaw control during hover and in low-speed flight. Forced air for the coanda slots and the aft thruster was provided by a variable pitch fan running at 5500 rpm.

h. Landing Gear

The Arapaho was designed with a retractable landing gear system consisting of two main landing wheels, a single tail wheel and a tail skid. The footprint of the landing gear was designed to make the helicopter suitable for shipboard operations. The landing gear incorporated a brake system and is suitable for ground taxi and landing rolls as well as other ground operations. The landing gear was designed to absorb the shock of vertical crash velocities up to 42 ft/sec to minimize the risk of injury to the aircrew during a crash.

i. Armament

The Arapaho was designed with an integrated weapon system utilizing Hellfire anti-tank missiles, Stinger air-to-air missiles, and a 30mm turreted cannon. The aircraft can carry eight Hellfire or Longbow-Hellfire missiles in internal weapons bays for the primary mission with the option to carry eight more missiles on external pylons for the

alternate mission. The design provided for the ability to carry and launch four Stinger missiles from pods on the wingtips.

III. CONSTRUCTION OF THE MODEL

The model was constructed in several sections or components. Sketches or drawings of each component were made using measurements from the design proposal [Ref. 3]. The components were then constructed in the shop. Required modifications were made based on visualization of the component or required fit to other components. The principal sections of the model were the main or forward fuselage, the wings, the tail section, the tail boom, the main rotor blades and rotor head, and the weapons systems.

A. FORWARD FUSELAGE

The main part of the forward fuselage of the model (Fig. 3.1) was constructed of three pieces of pine. The main block was four inches wide by seven inches high by 26 3/8 inches long. A 2 1/2-inch diameter 3-inch long round dowel was bolted to the rear of the main block (Fig 3.2) to be used as a mounting point for the tail boom. Two one-inch wide pieces of pine were added to each side of the main block to make a total width of six inches. Slots for the wings, to be mounted at a 15 degree angle of incidence, were cut in the side pieces and the pieces were glued to the main block. The shape of the canopy was then cut out of the forward fuselage to enable shaping of the nose section.

1. Nose Section

The nose section presented a difficult modeling problem. It was to be faceted to reduce the helicopter's radar signature, yet also needed to be streamlined aerodynamically.

Figure 3.1 Forward Fuselage

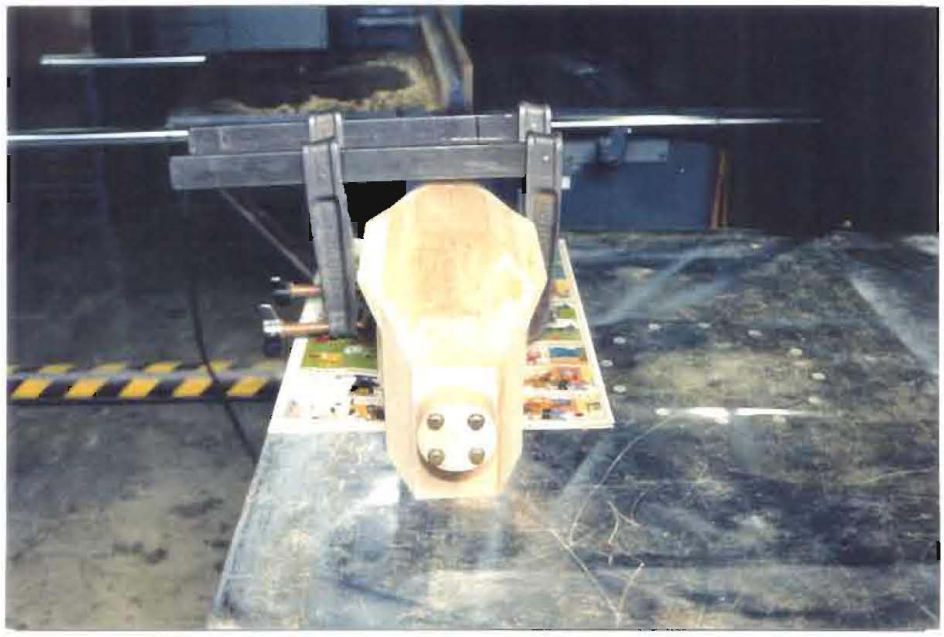

Figure 3.2 Tail Boom Attachment

Additionally, the Target Acquisition and Designation System/Pilot Night Vision System (TADS/PNVS) was to be mounted on the front of the nose. A series of cross-sections were cut from masonite and mounted on a keel beam (Fig. 3.3) in order to visualize the shape of the nose and forward fuselage. Once this was done, the nose was cut and sanded into shape. The TADS/PNVS was designed from the drawings shown in Figure 3.4. Modifications were made to the TADS/PNVS on the model for simplicity of construction, then it was glued to the nose of the fuselage.

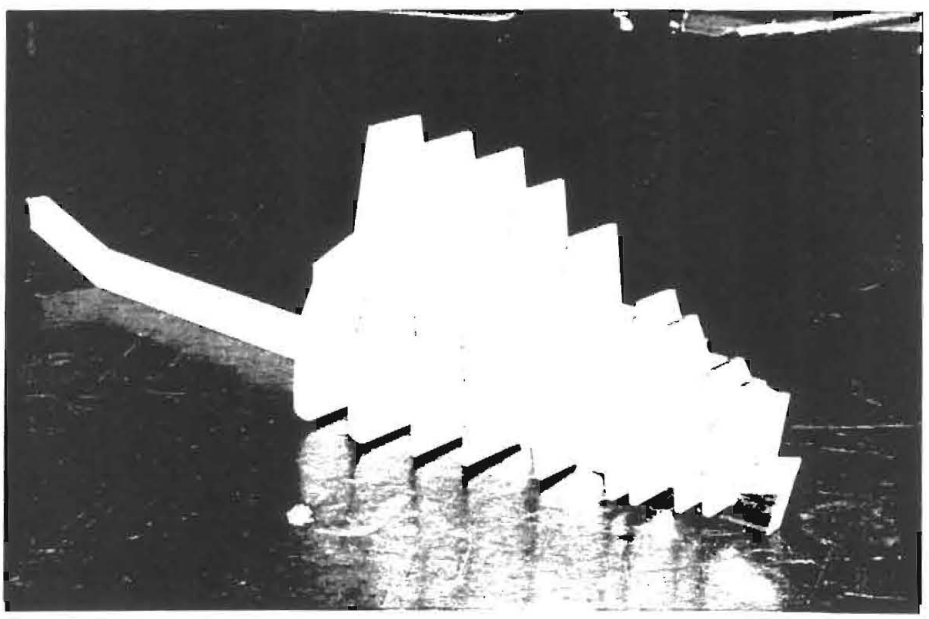

Figure 3.3 Masonite Section Model

2. Engine Intakes and Cowlings

Two 5/8 inch wide by 1 3/4-inch high by 9-inch long blocks were used to construct the engine cowlings. The intakes and cowlings had to be moved up the aircraft fuselage because the original design would have provided too much interference with the airflow over the wings. The wood blocks were secured to the fuselage by two wood

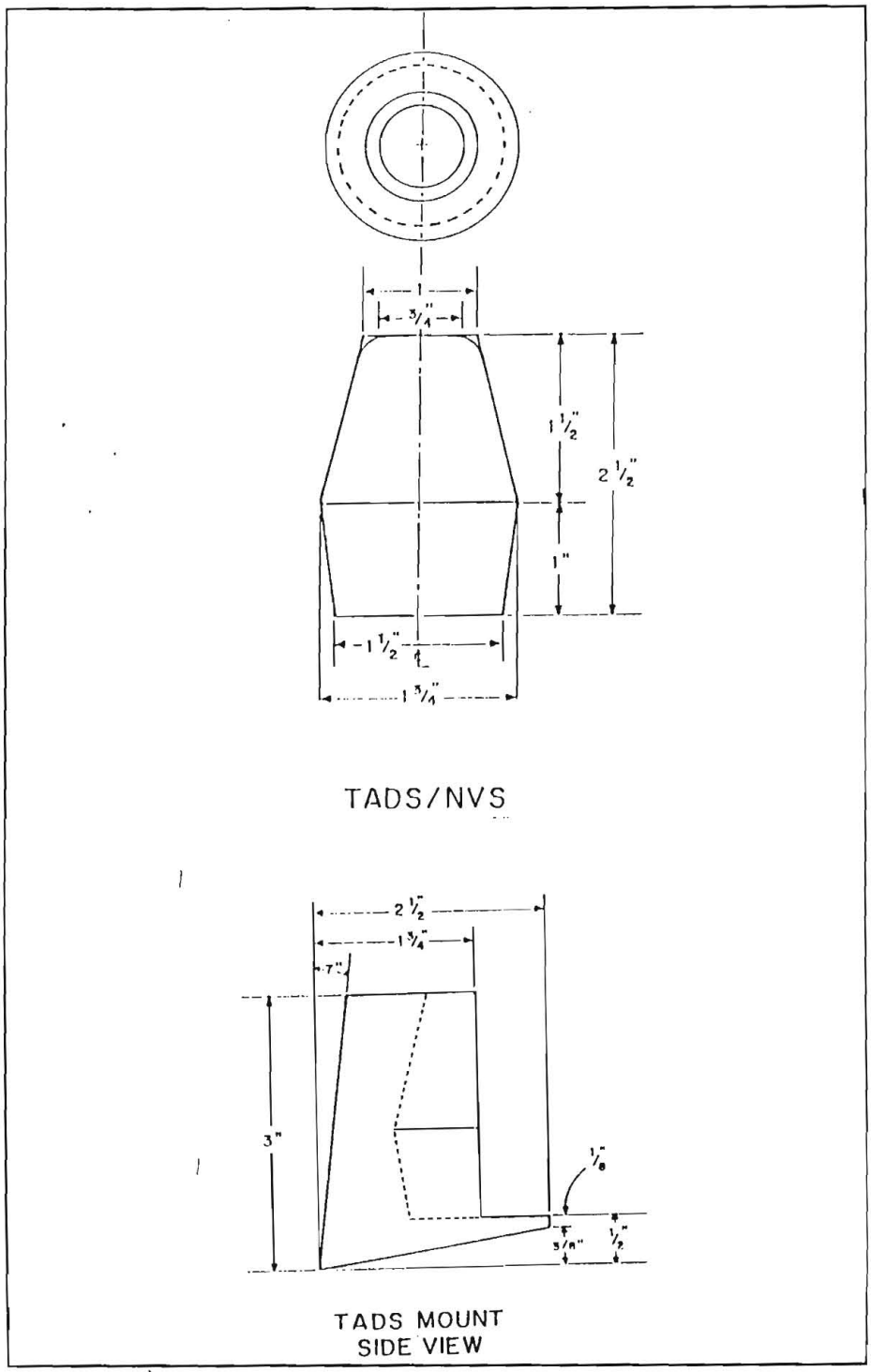

Figure 3.4 TADS/PNVS

screws. The triangular shape of the engine intakes and the final shape of the cowlings was produced, as shown in Figure 3.1, when the transmission deck and transition section was shaped.

3. Weapons Bay

The weapons bays were constructed from the drawing shown in Figure 3.5. The original design drawings did not accurately show the 15 degree angle of incidence of the wing causing a mismatch between the size of the weapons bays and the wing when the model was actually constructed. The solution was to position the weapons bays forward of their original design location in order to fit the entire weapons bay under the wing. Because of this move, a second piece of wood was needed to fill the space between the weapons bays and the nose section of the fuselage and to fair the forward part of the weapons bays into the fuselage, as shown in Figure 3.1.

4. Canopy

The canopy was constructed from a single piece of wood and shaped to mate with the forward fuselage. There was a discrepancy in the various views of the canopy in the original design and the canopy had to be constructed twice in order to get it right. Several drawings were made of various shapes prior to deciding on a final shape. The object was to stay as close to the original design but make it functional. The first canopy that was constructed turned out to be too narrow, which would have left very little room for a human's shoulders. The second and final canopy was wider and constructed from the drawing in Figure 3.6.

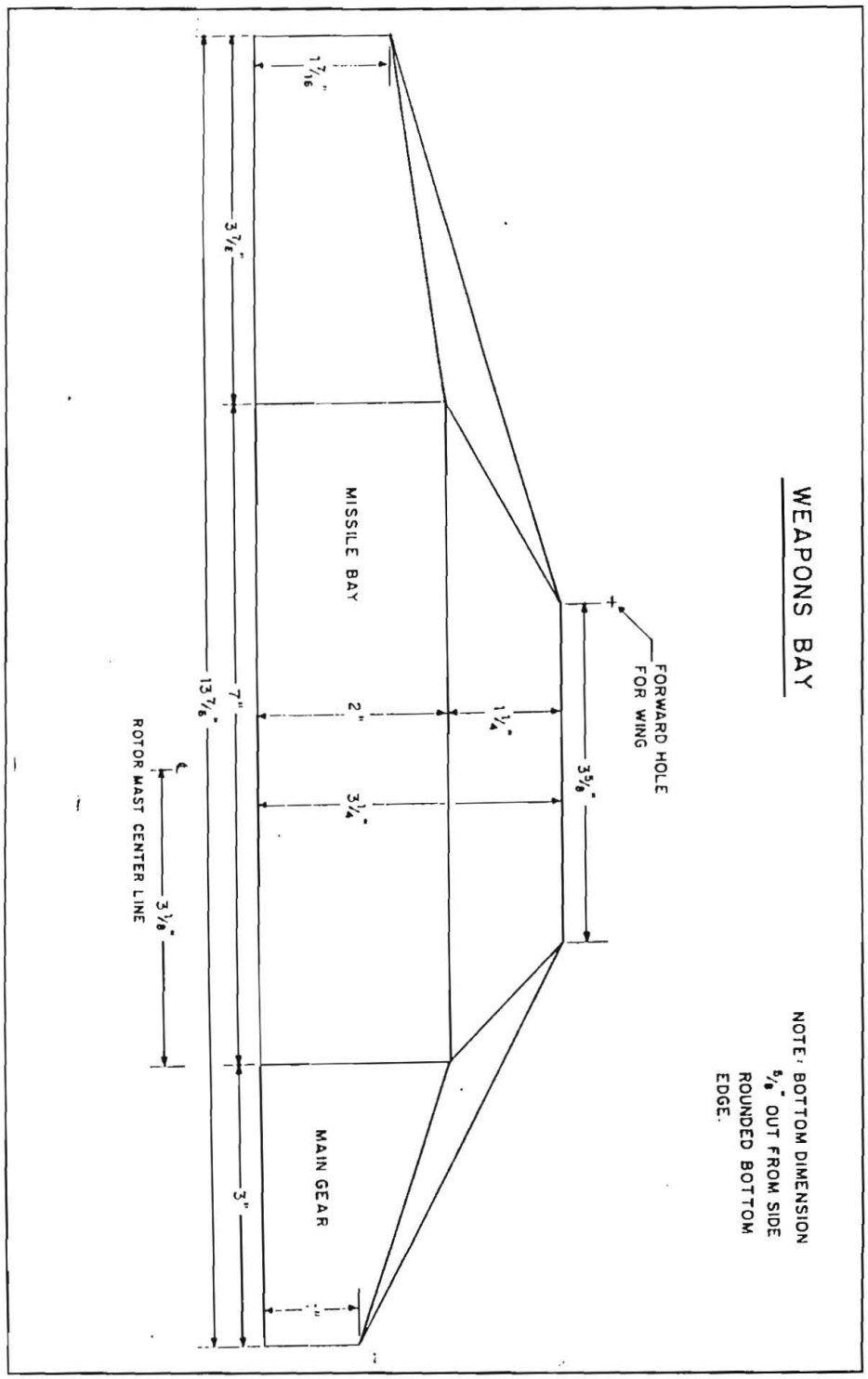

Figure 3.5 Weapons Bay

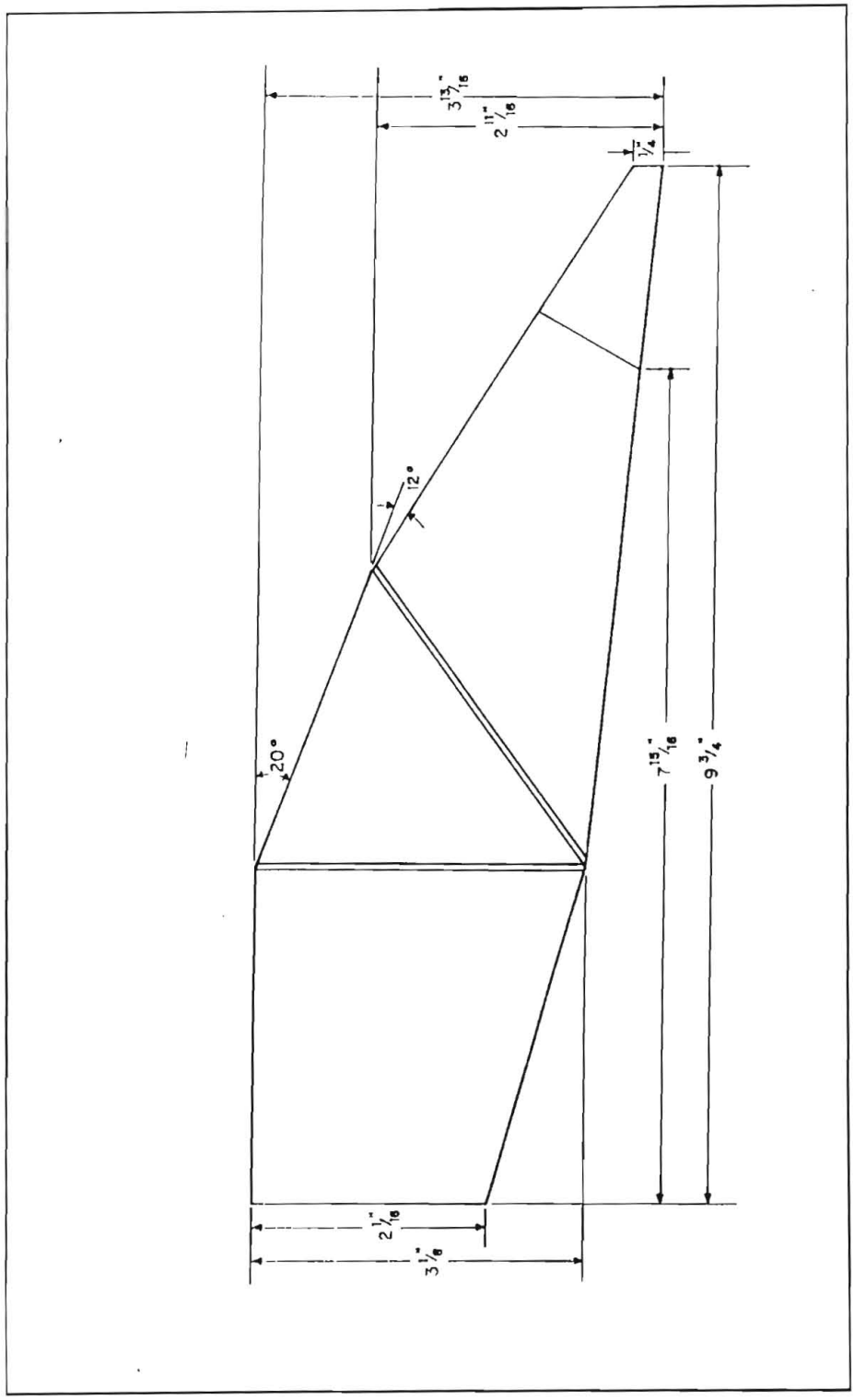

Figure 3.6 Canopy

5. Final Shaping of the Fuselage

Once all the components of the fuselage were constructed and assembled, the final shaping was completed. Before the canopy was glued to the forward fuselage, the shape of the nose was finalized and sanded into shape, and the area just aft of the canopy was faired into the engine intake area and the forward transmission deck. The canopy was then glued into place and faired into the nose section and the TADS. Finally the transition section, the rear of the main fuselage, was faired from the flat surfaces of the transmission deck, the sides and the bottom to the rounded shape of the tail boom producing the finished product shown in Figure 3.1.

B. TAIL BOOM

The tail boom was 21 3/4 inches long from the junction with the main fuselage to the rear tip of the NOTAR™ thruster can. It was constructed from a 21 3/4-inch long, 2 3/4-inch diameter plexiglas tube, two cardboard tube spacers, and a 3-inch diameter galvanized steel sheet metal stovepipe as shown in Figure 3.7. The plexiglas tube was installed over the 2 1/2-inch dowel at the rear of the main fuselage, as shown in Figure 3.8. The bottom rear of the stovepipe was cut to produce the shape shown in the original design. The cardboard spacers and steel stovepipe were then slipped over the plexiglas tube producing the oval shape of the NOTAR™ tail boom. A slot was cut in the upper side of the tail boom to allow for the mounting of the horizontal and vertical tail section. A plug was installed in the rear of the plexiglas tube to close the tail boom.

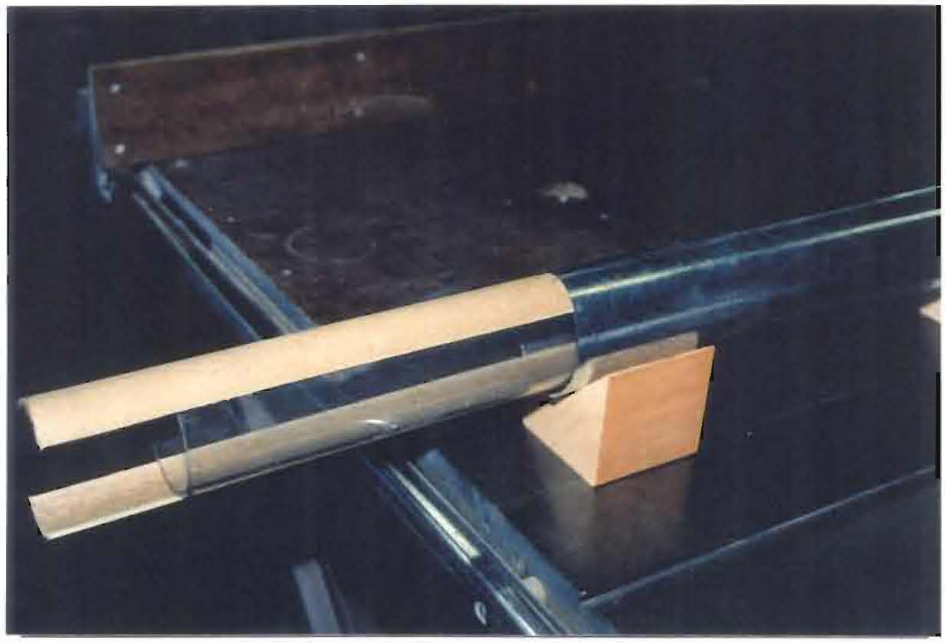

Figure 3.7 Tail Boom Components

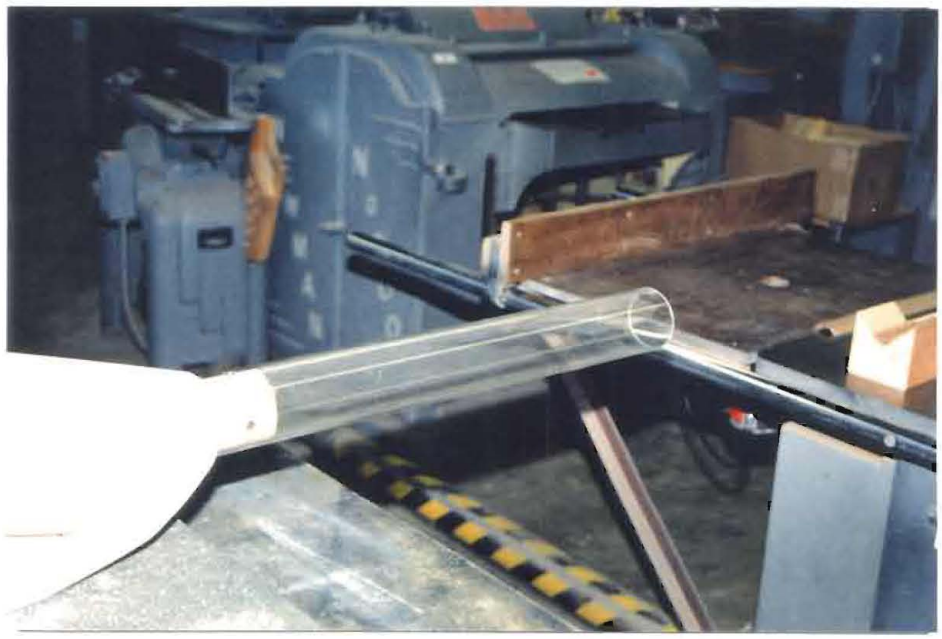

Figure 3.8 Tail Boom Assembly

C. WINGS

The wings were constructed from the drawing shown in Figure 3.9, minus the missile housing, which was added later. A NACA 64-012 wing section was used. A section template was made for the wing tip and the wing root. The wing planform was cut from a block of pine and the section templates glued to their respective ends. The wings were then sanded to the final shape. An attachment plate was connected to the wing root in order to attach the wings to the main fuselage. The wings were then mounted on the fuselage at a 15 degree nose up angle. The relatively high angle of the wing was needed to compensate for rotor downwash and fuselage forward tilt at 200 knots while providing 3500 lbs. of lift.

D. VERTICAL AND HORIZONTAL TAIL

The vertical tail and horizontal stabilator were constructed from pine using the drawings shown in Figures 3.10 and 3.11 respectively. The tail sections were constructed in the same manner as the wings. The vertical tails were connected to the horizontal, as in Figure 3.12, by glue and wood screws for strength. Two holes were pre-drilled in the horizontal tail section in order to mount the entire tail section to the tail boom, as shown in Figure 3.13.

E. ROTOR SYSTEM

The rotor system consists of two sets of parts, the rotor blades and the rotor hub.

1. Rotor Hub

The rotor hub was from a modified scale model remote control helicopter. The pitch change rods were removed to make the design cleaner and provide a simpler method

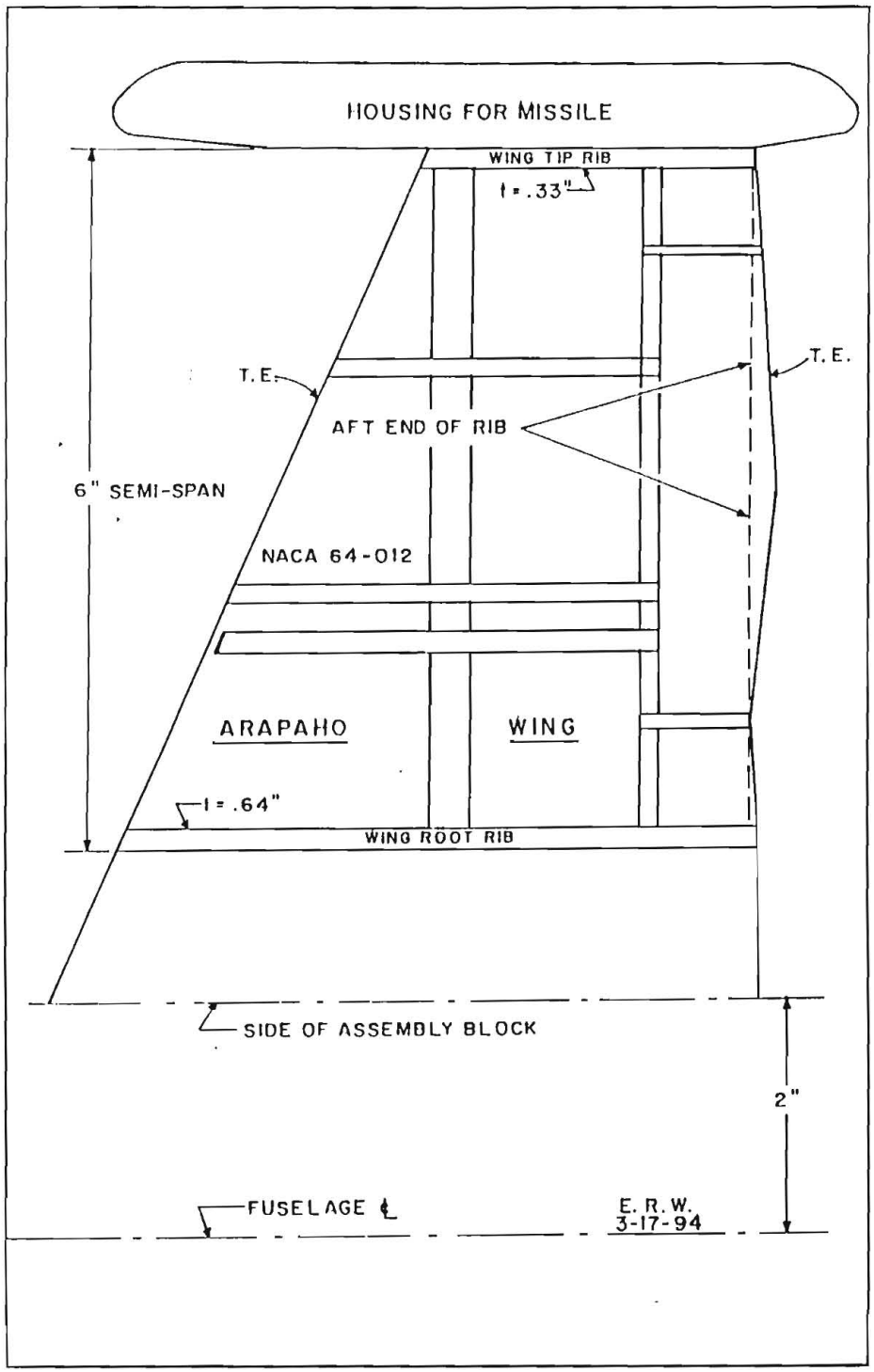

Figure 3.9 Wings

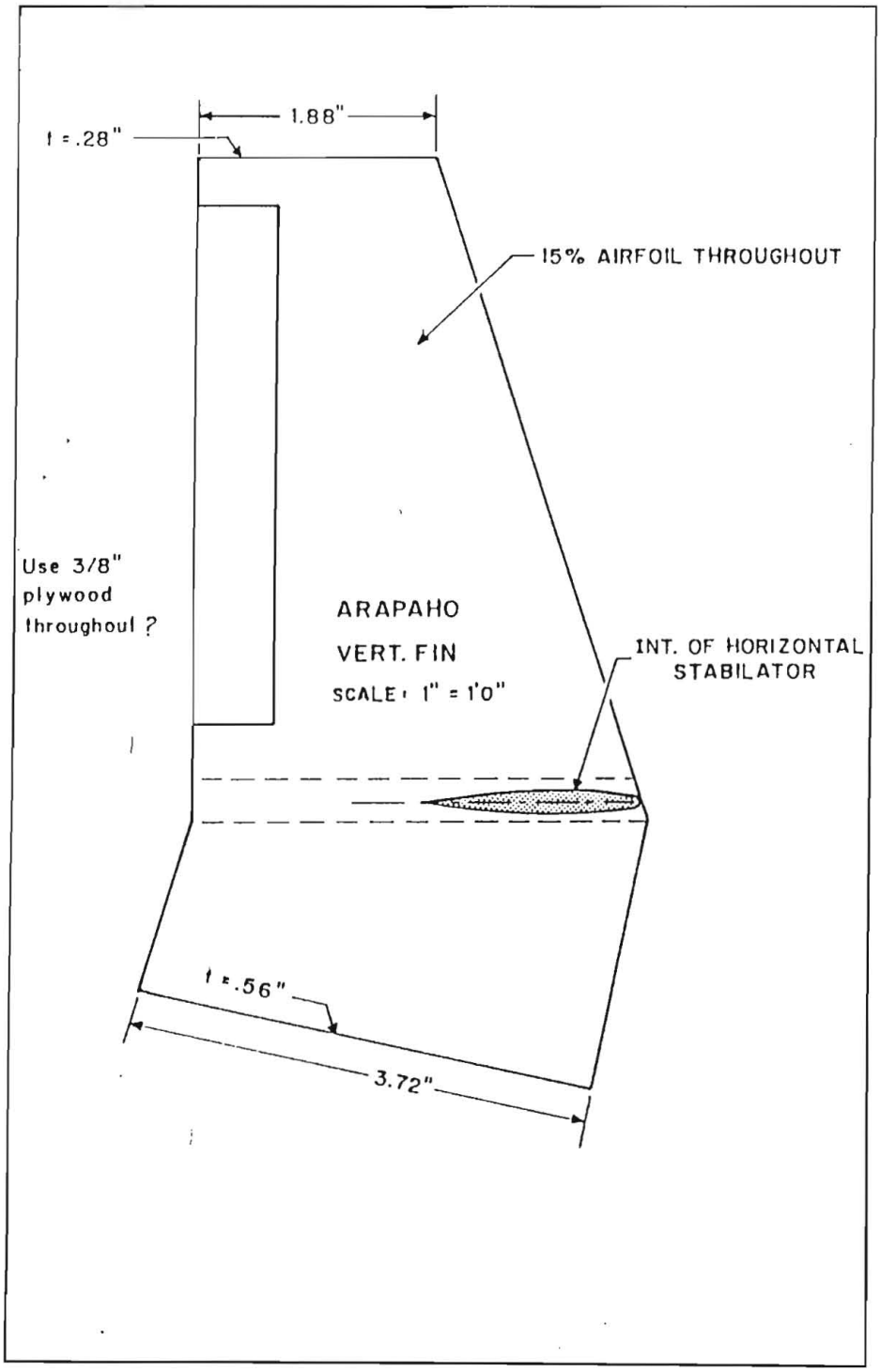

Figure 3.10 Vertical Tail

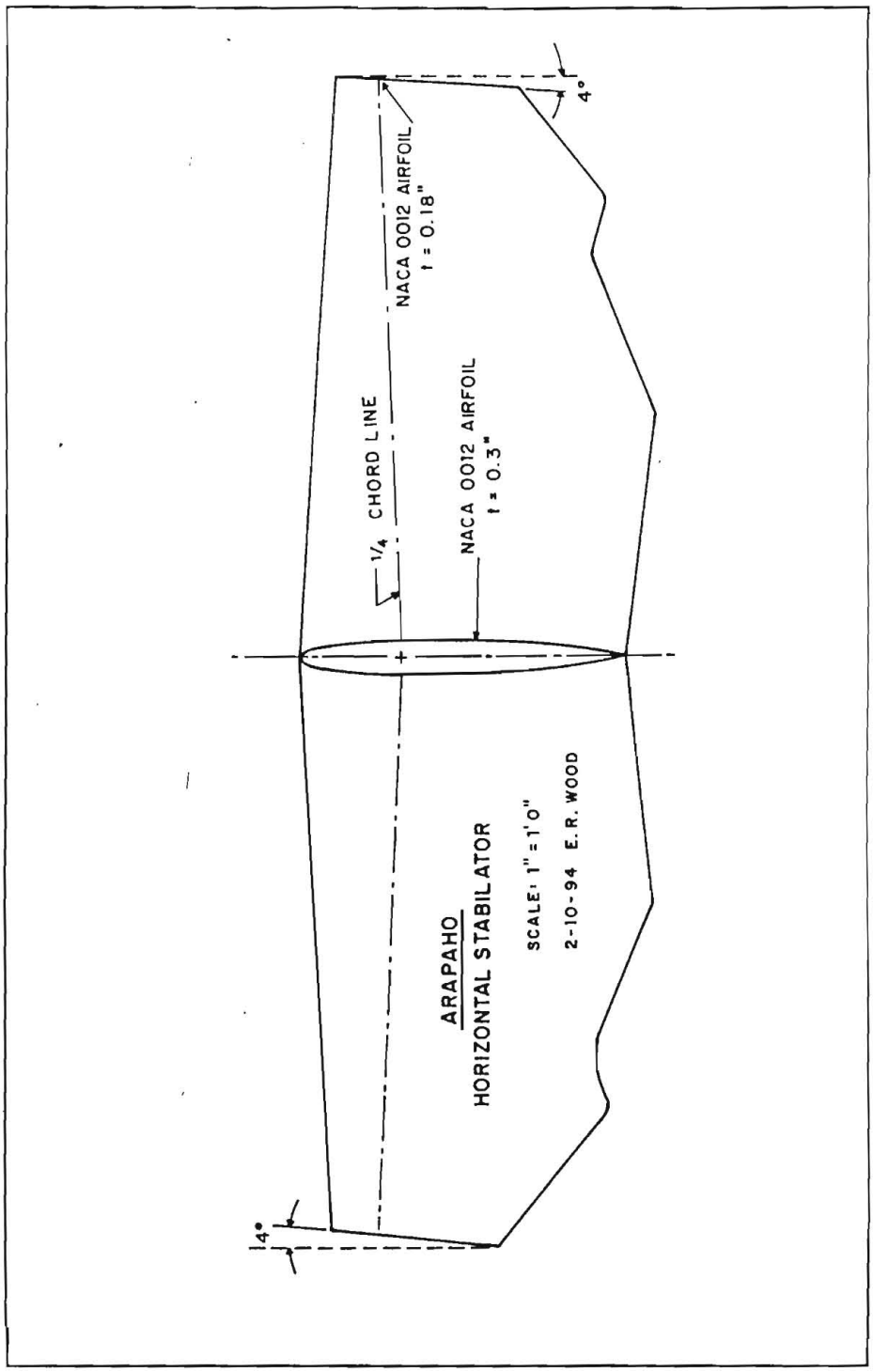

Figure 3.11 Horizontal Stabilator

Figure 3.12 Assembled Tail

Figure 3.13 Mounted Tail Section

to mount the hub on the main fuselage. The rotor system was mounted on the fuselage by drilling a 3/8-inch hole in the top of the fuselage where the rotor system was to be mounted, and the shaft of the rotor hub was inserted into the hole.

2. Rotor Blades

Each rotor blade was constructed from a single piece of pine. The blades were 24 inches long with a hub attachment block at the root and 20 degrees aft sweep at the tip, shown in Figure 3.14. The section was matched as closely to the Boeing VR-12 blade section as was possible.

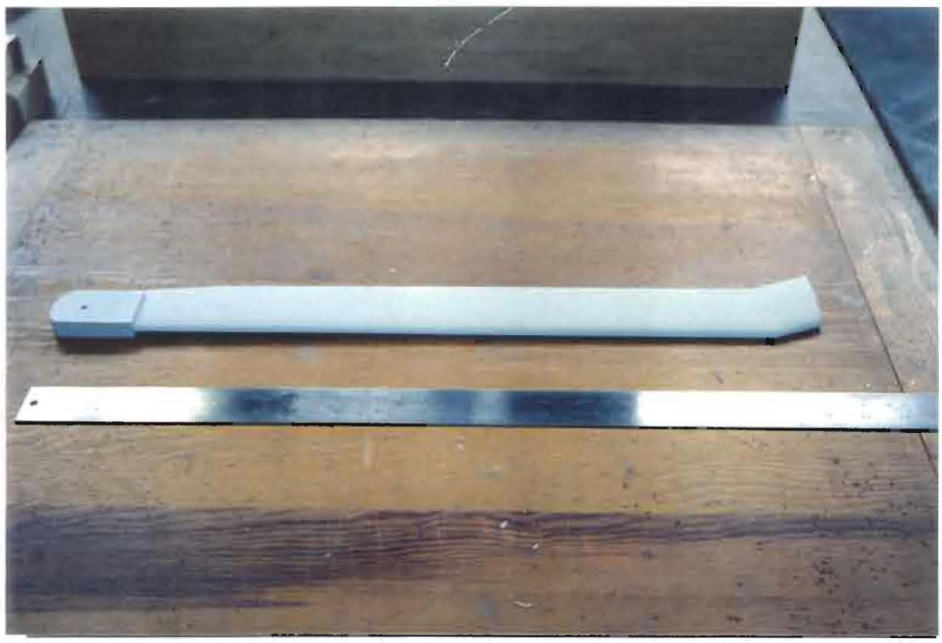

Figure 3.14 Rotor Blades

F. WEAPON SYSTEMS

The weapon system was comprised of a gun turret, Stinger Air-to-Air missile pods, and the Longbow radar. The gun turret and the Stinger pods were constructed from

wood using the drawings shown in Figures 3.15 and 3.16, while the Longbow radar was constructed using scaled dimensions provided by McDonnell Douglas Helicopters.

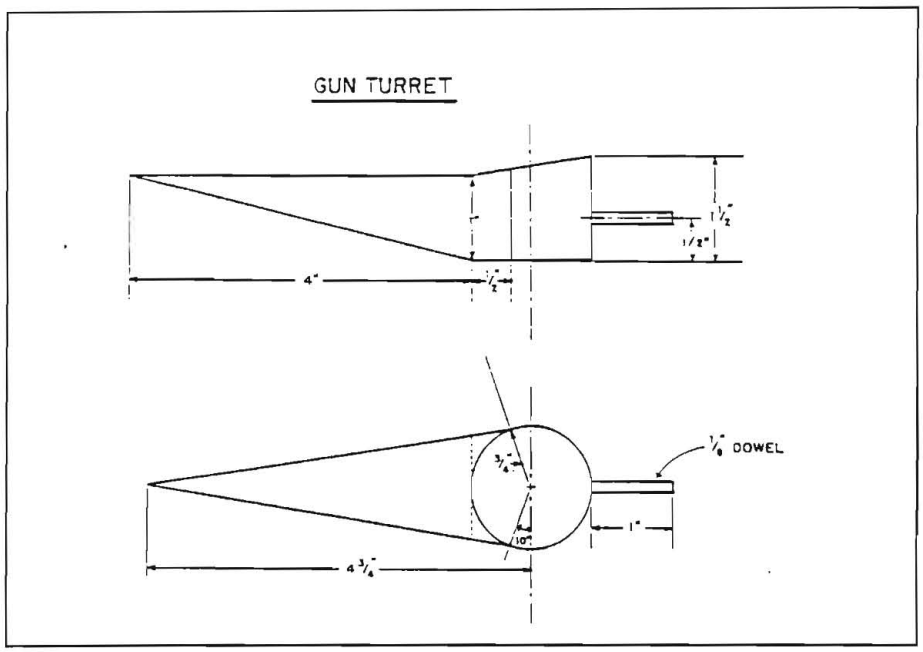

Figure 3.15 Gun Turret

1. Longbow Radar

The Longbow radar was mounted on top of the main rotor hub by an aluminum rod, as shown in Figure 3.17. The Longbow radome was slipped over the mount and secured with a set screw.

2. Stinger Pods

The Stinger pods were mounted on the wing tips and secured by a wood screw and wire brad on each pod. The pods were mounted in a level attitude as in the original design.

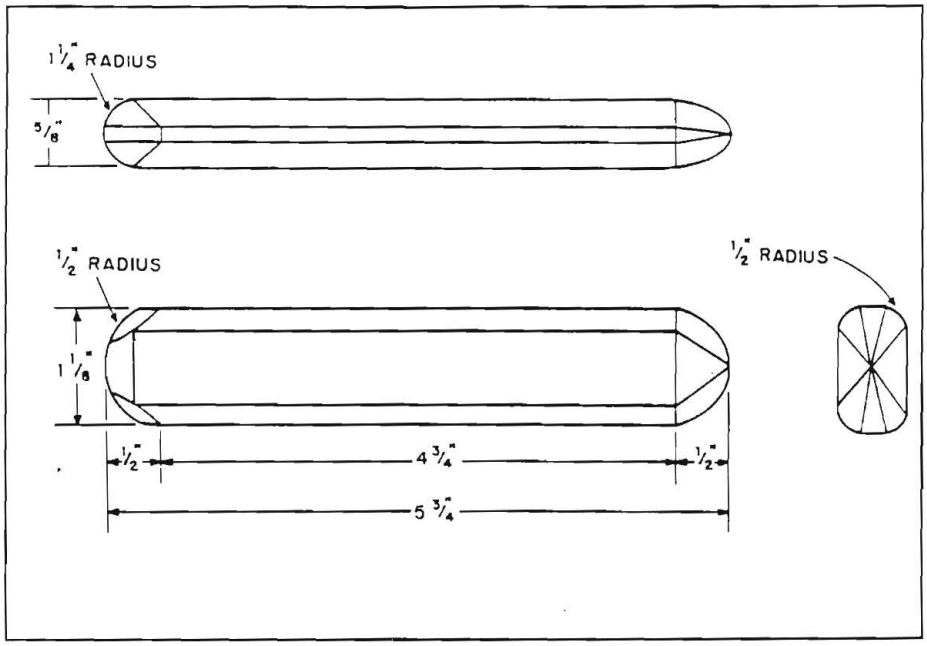

Figure 3.16 Stinger Pods

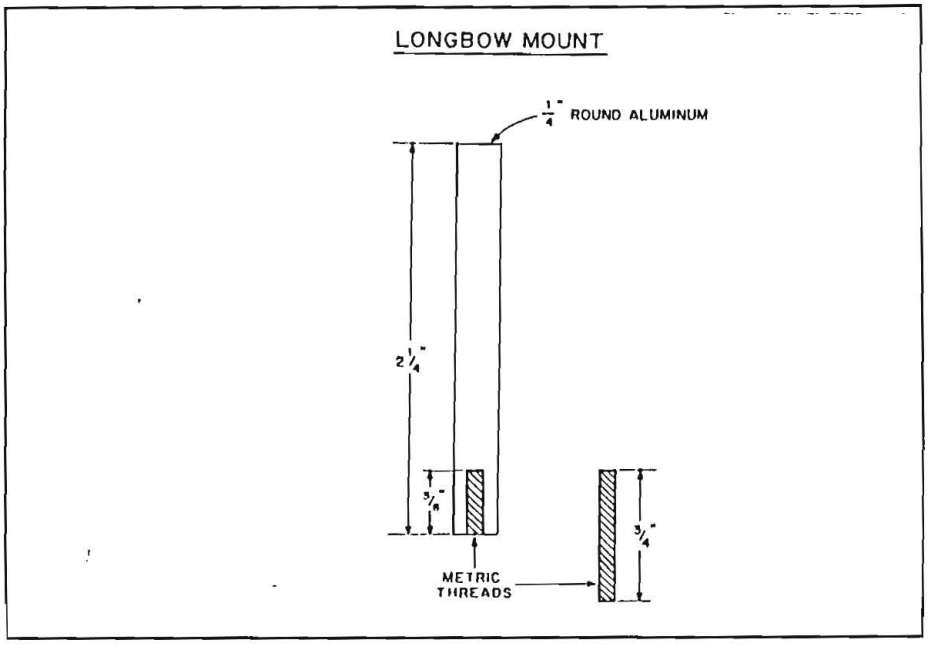

3.17 Longbow Radome Mount

3. Gun Turret

The gun turret was constructed in three pieces, the turret, the fairing, and the gun barrel. On the final model, the gun barrel was enlarged from the initial model dimensions to 1 1/2 inches long and 1/4-inch diameter, in order to improve scaling of the gun. The turret was assembled and glued to the underside of the nose of the main fuselage.

G. FINAL ASSEMBLY

Once all the individual parts were fabricated, the completed model was assembled. The tail boom was connected to the main fuselage, then the tail section was secured to the top of the tail boom by two wood screws, and the gun turret was glued to the underside of the nose of the main fuselage. The wings were then installed and putty was used to seal any seams, cracks, or imperfections. The model and remaining parts were sanded and painted with several coats of primer. Then the entire model was painted olive drab. The canopy was trimmed in olive drab and painted light blue with a speckling of white to give the impression of glass. Black trim was added to the model using a thin line permanent felt tip marker. The model was completed by applying "U.S. Army" decals to the tail boom. The completed model is shown in Figure 3.18.

Figure 3.18 Completed Model

IV. EXPERIMENTAL PROCEDURE

A. PREPARATION

In preparation for testing the 1/12th scale model of the Arapaho, the wind tunnel blockage effects were calculated, the estimated lift and drag of the model were calculated, a data acquisition system was set up, the wind tunnel balance table calibration was checked, and the model mounted in the wind tunnel.

1. Blockage Effects

The presence of the model in the wind tunnel test section produces what are known as "blockage effects". [Ref. 4, pp. 268-291] Blockage effects can be broken down into two types: solid and wake blocking. Solid blocking is due to the reduction in cross-sectional area of the wind tunnel test section which increases the air velocity increases as it flows over the model. Wake blocking is due to the different velocities of the air flow inside and outside of the wake behind the model. The velocity of the air flow outside the wake of the model is higher than both the air inside the wake and the freestream, producing lower pressure and increased drag. Before testing the Arapaho model in the NPS low speed wind tunnel, the ratio of model frontal area to test sectional area was calculated. A maximum ratio of 7.5 percent is considered an acceptable limit to minimize errors [Ref. 5, p. 326]. The ratio of frontal area of the Arapaho model to the NPS low speed wind tunnel test section cross-sectional area was 3.2 percent. Then the combined effect of solid blocking and wake blocking was determined by:

$$\varepsilon = .25 \times \frac{\text{model frontal area}}{\text{test section area}} \tag{4.1}$$

For the Arapaho model in the NPS low speed wind tunnel, $\varepsilon = .00817$.

2. Lift Estimation

First the lift that would be generated by the model at various airspeeds was calculated in order to estimate the forces that would be acting on the model stand and table balance. The following equations were used to calculate the lift forces:

$$L = C_l \times q_\infty \times A_W \tag{4.2}$$

where:

L = lift

q_∞ = dynamic pressure

C_l = wing lift coefficient

A_W = wing area

and

$$q_\infty = \tfrac{1}{2} \times \rho \times V^2 \tag{4.3}$$

where

ρ = air density in slugs/ft^3

V= velocity in ft/sec

The total wing area for the Arapaho Model is 48.75 in^2 or 0.3854 ft^2. Standard day sea level air density was used. Lift forces were calculated for airspeeds of 20, 40, 50, 60, and 70 knots in order to cover the range of airspeeds to be tested in the wind tunnel. The results are shown in Table 4.1.

Velocity (knots)	Lift (lbf)
20	0.64
30	1.45
40	2.57
50	4.02
60	5.79
70	7.88

Table 4.1 Model Generated Lift

3. Drag Estimation

Estimation of the drag on the model was a much more complicated process. The equivalent flat plate area of both the model and the full scale aircraft were estimated by the method described in Prouty [Ref. 3, pp. 305-308] and the US Air Force Datcom Manuals. The solution was obtained by first separating the body into smaller units, such as, fuselage, wings, engine nacelles, horizontal stabilator, vertical tail, and missile pods; then calculating the equivalent flat plate area of each unit and adding them all together. Induced drag produced by the lift generated by the wings, horizontal stabilator, and vertical tails was accounted for in the calculations. Additionally, the equivalent flat plate area of the Longbow radome and the rotor hub was calculated. Table 4.2 shows a comparison of the estimated equivalent flat plate areas.

Subsection	Model	Aircraft
Fuselage	0.02	2.55
Engine Nacelles	0.004	0.57
Horizontal Stab	0.009	0.72
Vertical Tail	0.077	10.33
Stinger Pods	0.0006	0.05
Wings	0.079	12.28
Total	0.191	26.5
Rotor Hub	0.045	6.7
Longbow Radar	0.028	4.09

Table 4.2 Estimated Equivalent Flat Plate Area (Sqft)

4. Data Acquisition Setup

The NPS low speed wind tunnel was constructed with an integral strain gage balance and turntable [Ref. 6]. The balance and turntable apparatus is floor mounted below the wind tunnel test section. The top of the apparatus is the base to which the models are mounted in the test section of the wind tunnel. There is a chain and gear mechanism at the bottom of the turntable connected to an electric motor which enables the turntable to be remotely turned in either direction. The signal from the strain gages, operating on a 10 Vdc power supply, were fed, through a locally produced signal conditioner, to a Fluke 8050A Digital Multimeter. The signal conditioner provided both the 10 Vdc power for the operation of the strain gage bridges, and the controls necessary to calibrate and zeroize the readings. Data readings were taken in millivolts accurate to two decimal places from the Multimeter. This setup allowed the measurement of the axial and normal forces and the axial and normal moments acting on the model. The primary force of interest was the axial force acting on the model from which the drag force was calculated.

5. Balance Calibration

Before any tests were conducted, it was necessary to make a check of the calibration of the balance completed previously. [Ref. 6, p.102] The calibration apparatus, shown in Figure 4.1, was used and several data points were measured and compared to the previous balance calibration. The data points matched the previous calibration runs, confirming the accuracy of the calibration matrix shown below.

$$K=\begin{bmatrix} 8.3714 & -4.9115 & 1.0564 & -1.6847 \\ -13.998 & 164.5562 & -22.3346 & 38.426 \\ -0.5946 & 1.7055 & 9.9066 & -5.5392 \\ 10.466 & -36.3139 & -50.1701 & 169.2285 \end{bmatrix} \tag{4.4}$$

6. Mounting the Model

A stand was built to mount the Arapaho model in the level flight configuration and is shown in Figure 4.2. This mount provided minimum tare and interference, while providing a steady platform to mount the model to the balance table. This method of mounting was chosen because of the availability of hardware, the size and weight of the model, and the simple interface with the wind tunnel strain gage balance table. However, mounting the model in this fashion limited the tests to the use of a level attitude and ruled out the ability to obtain any lift data. The level attitude limit imposed little restriction on the tests since the helicopter flight schedule called for level flight throughout most of the 1g flight envelop. The model was then mounted on the stand as shown in Figures 4.3, and 4.4.

B. TEST RUNS

Once preparations were completed, wind tunnel runs commenced. Six data runs were completed: one run with just the model stand, two runs with the model mounted in

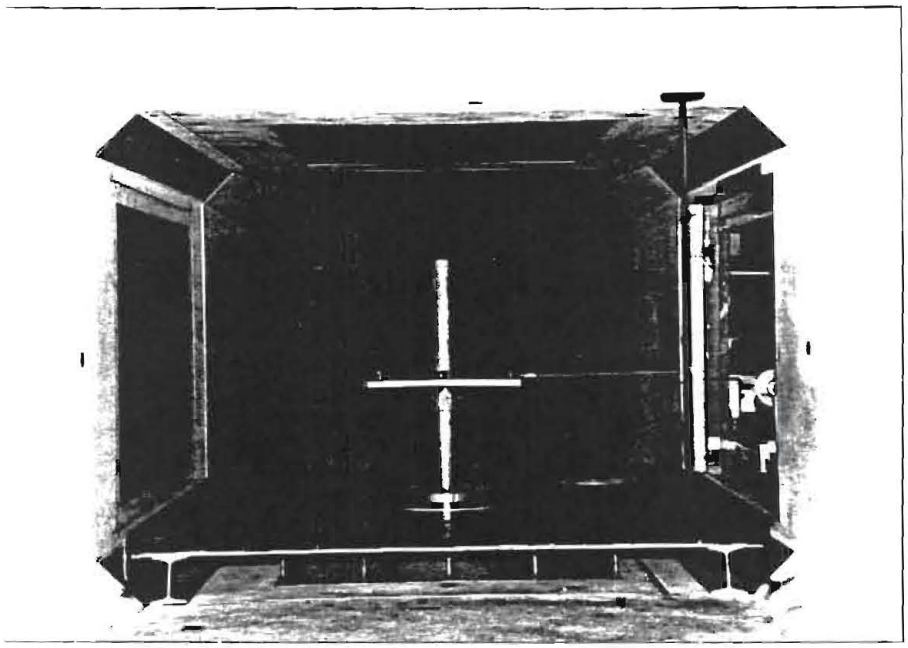

Figure 4.1 Balance Calibration Apparatus

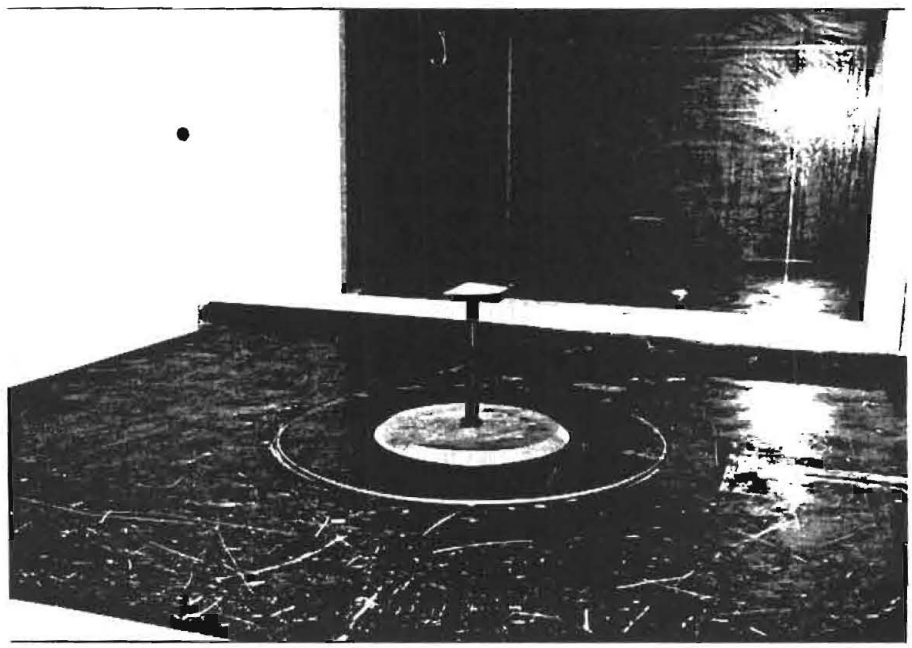

Figure 4.2 Model Stand

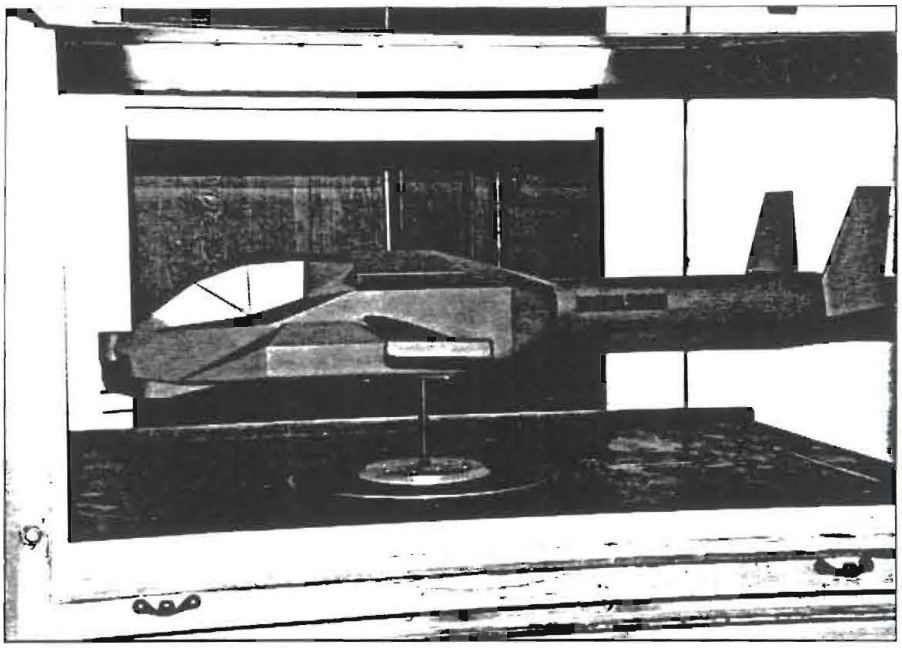

Figure 4.3 Mounted Model

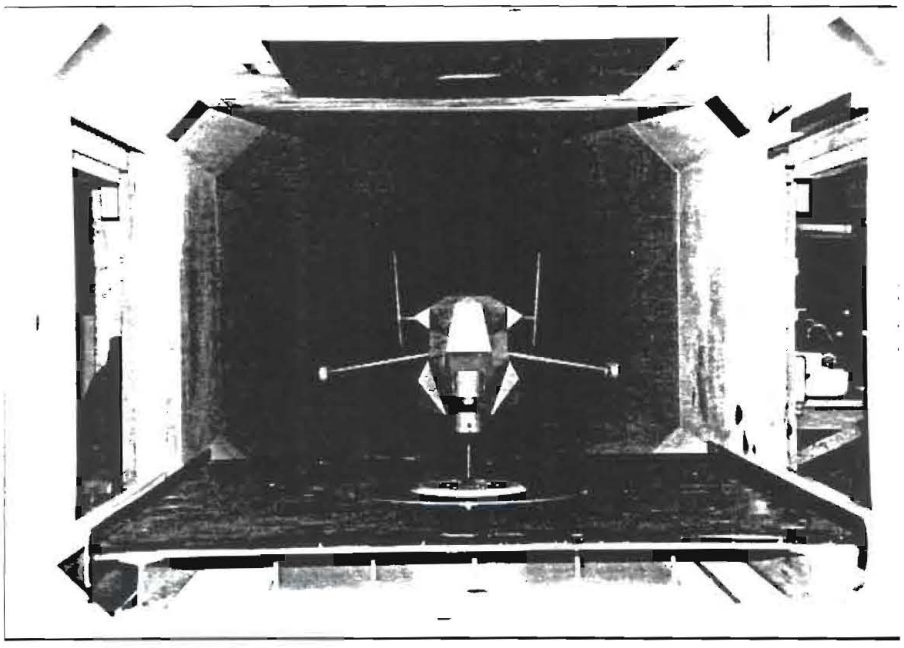

Figure 4.4 Model in Wind Tunnel

the wind tunnel, one run with the rotor hub installed, one run with both the rotor hub and the Longbow radome installed, and one run of the model with rotor hub and Longbow radome at various yaw angles up to 10 degrees. The first three runs were run at velocities from approximately 20 knots to approximately 70 knots. The next three runs were run at velocities from approximately 30 knots to approximately 55 knots. The data measured during the runs are shown in Tables A.1, A.2, A.3, A.4, A.5, and A.6 in Appendix A.

1. Test Section Velocity

a. Velocity Measurement Devices

The NPS wind tunnel has two devices for measuring test section velocity. The first is a pitot tube located in the upper left hand corner of the test section. The pitot tube is connected to an aircraft-type airspeed indicator that gives an instantaneous but approximate test section airspeed. This system was used to set and adjust the approximate wind tunnel blade pitch settings. The second system uses an integral water manometer to accurately determine test section velocity. There are pressure pick-ups in the settling chamber and the throat of the test section and the pressure differential, in centimeters of water, between the settling chamber of the wind tunnel and the test section is measured using the water manometer. This pressure differential is used to accurately set the test section freestream velocity.

b. Velocity Calculation

The approximate wind tunnel velocity is set using the airspeed indicator, then any small refinements are made using the water manometer. The pressure differential, ΔP,

is measured and recorded. The pressure differential is then converted to lb/ft^2 by the following equation [Ref. 7, p. 17]:

$$\Delta P(lb/ft^2)=\Delta P(cm\ H_2O)\times\gamma_{water}\times .03281 ft/cm \tag{4.5}$$

where

$$\gamma_{water}=62.35\ lb/ft^2 \tag{4.6}$$

The pressure differential is then converted to test section velocity, V_∞, by combining the wind tunnel calibration equation (4.7), which was previously determined (9 May 94),

$$\Delta P=0.913\times q_\infty \tag{4.7}$$

with the dynamic pressure equation

$$q_\infty=\tfrac{1}{2}\times\rho\times V^2 \tag{4.8}$$

and rearranging to give

$$V_\infty(ft/sec)=\sqrt{\frac{2\times\Delta P}{.913\times\rho}} \tag{4.9}$$

c. Velocity Corrections

The wind tunnel test section freestream velocity, V_∞, was then corrected for blockage effects, as described earlier, to give V_C. Equation 4.10 shows the method for blockage correction.

$$V_C=(1+\varepsilon)\times V_\infty \tag{4.10}$$

2. Data Collection

Six test runs were conducted and raw data was collected. The forces acting on the model were transmitted to the wind tunnel strain gage balance and were recorded manually as voltage readings on the multimeter. Before each run, the strain gage readings were zeroed out at zero airspeed. The data collected on each of the six runs, shown in appendix A, was converted from millivolt readings to forces and moments by use of equation 4.11 [Ref. 6, pp. 98].

$$[K] \times \begin{bmatrix} Eaa \\ Eba \\ Ean \\ Ebn \end{bmatrix} = \begin{bmatrix} \text{Axial Force} \\ \text{Axial Moment} \\ \text{Normal force} \\ \text{Normal Moment} \end{bmatrix} \tag{4.11}$$

Of primary interest was the Axial Force reading, which represents the drag force along the longitudinal axis of the model in all cases except run number six where the model was positioned at various yaw angles. In run six, the components of the Axial Force and the Normal Force in the direction parallel to the freestream direction were combined to find the drag force on the model. The equivalent flat plat area was then determined by dividing the drag by the dynamic pressure, as described earlier, using equation 1.1.

a. Model Stand

The model stand was mounted by itself in the wind tunnel, as shown in Figure 4.2, for the first run to obtain the tare. Aerodynamic interference coupling of the small model stand was estimated to be negligible and was neglected in the drag calculations. The wind tunnel velocity was varied from zero airspeed to 133.96 ft/sec (79.3 knots). The raw data is shown in Table A.1 in Appendix A. The drag and equivalent flat plate area are plotted versus velocity as shown in Figure 4.5. The average equivalent flat plate area for the stand alone was 0.029 ft^2 .

b. Model Fuselage

Two test runs were conducted with the basic model mounted on the stand in the wind tunnel as shown in Figure 4.4. This was done to determine the equivalent flat plate area of the fuselage itself. The wind tunnel velocity was increased slowly, in small increments to ensure the structural integrity of the model. A small vibration started at

approximately 60 ft/sec (35 knots) and increased slightly with increasing speed, but did not pose any problem to the test or the structural integrity of the model. The maximum velocity attained during these two runs was 118.78 ft/sec (70.3 knots). The data collected during these two runs is shown in Tables A.2 and A.3 in Appendix A. The drag and the equivalent flat plate area are plotted versus velocity in Figures 4.6 and 4.7 for each of the runs. The average equivalent flat plate area for the two runs combined was 0.23821 ft^2.

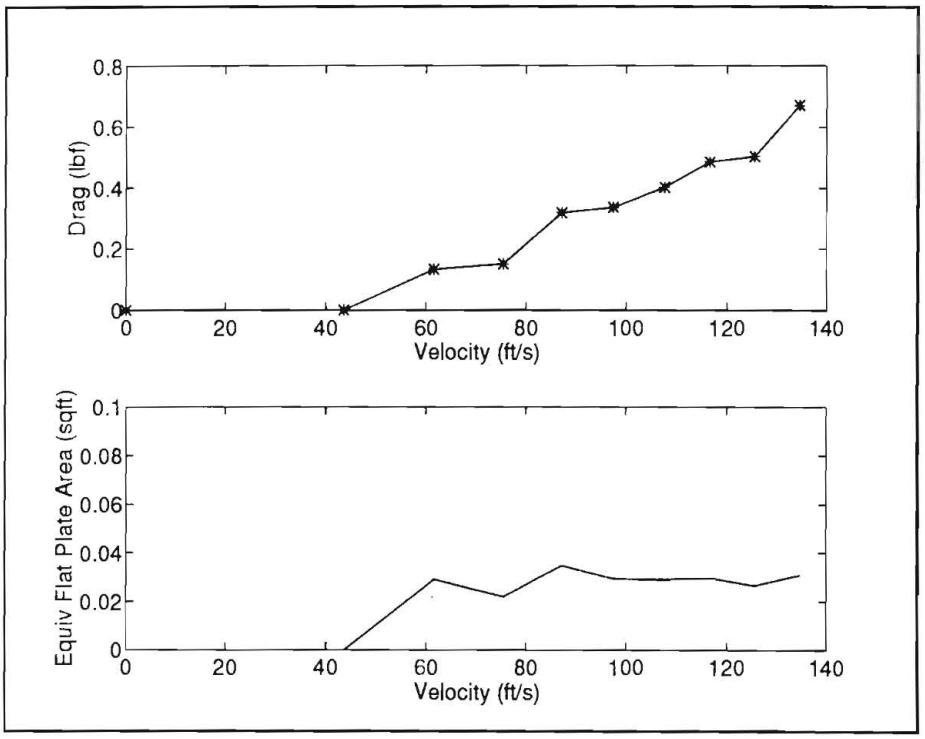

Figure 4.5 Drag and Equivalent Flat Plate Area, Stand Alone

c. Model with Rotor Hub and Longbow Radome

For the next two runs, the rotor hub and the Longbow radome were installed, one at a time, to compare the change in drag from the basic fuselage. Figures 4.8 and 4.9 show the configuration during the respective runs. The maximum velocity in these two runs was 93.6 ft/sec (55.4 knots) and the data is recorded in Tables A.4 and A.5 in

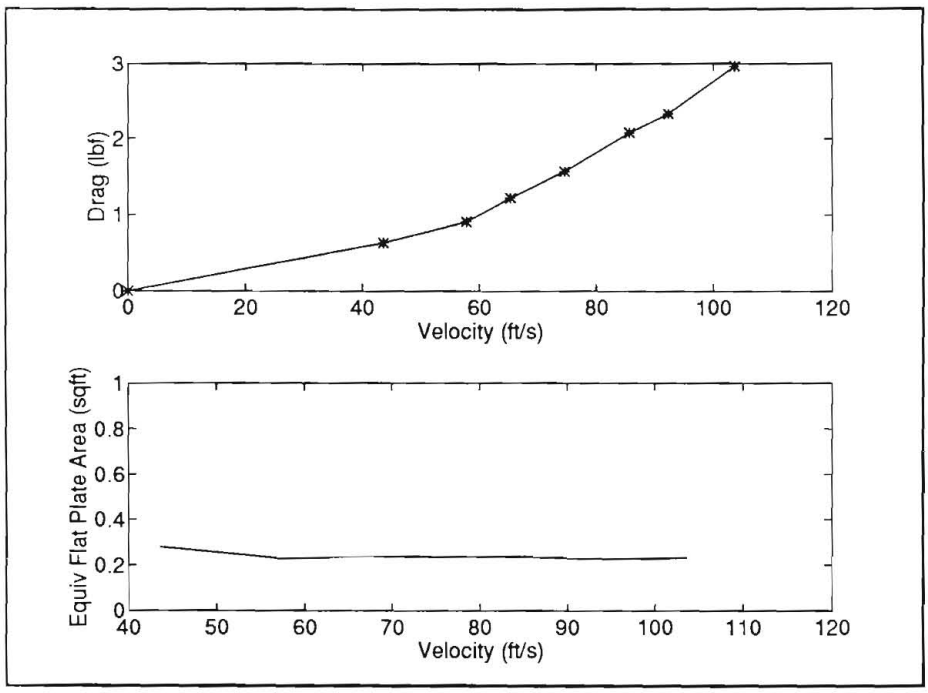

Figure 4.6 Drag and Equivalent Flat Plate Area, Basic Model - Run 1

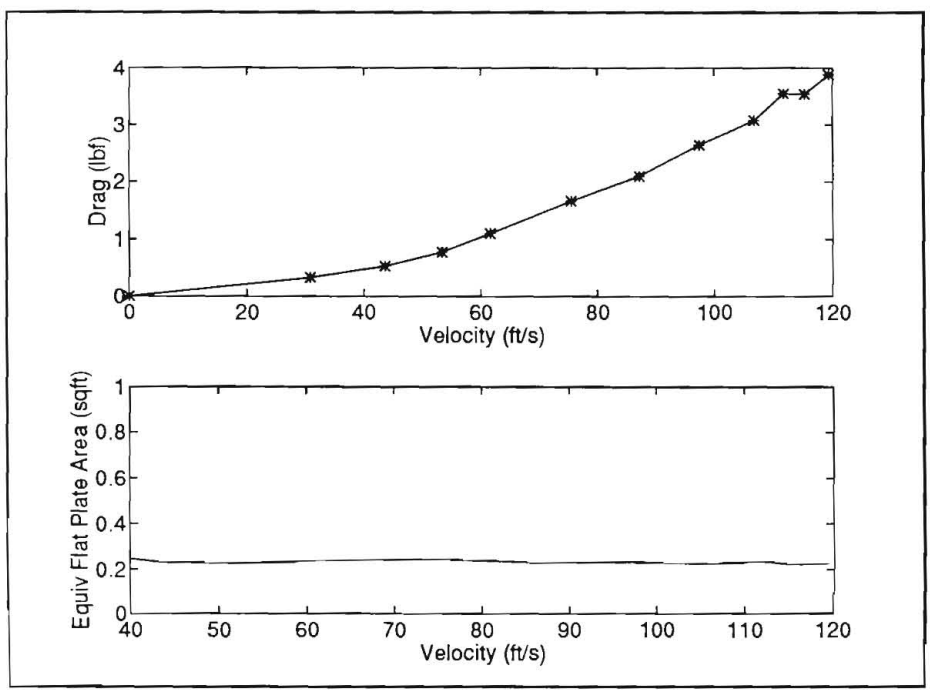

Figure 4.7 Drag and Equivalent Flat Plate Area , Basic Model - Run 2

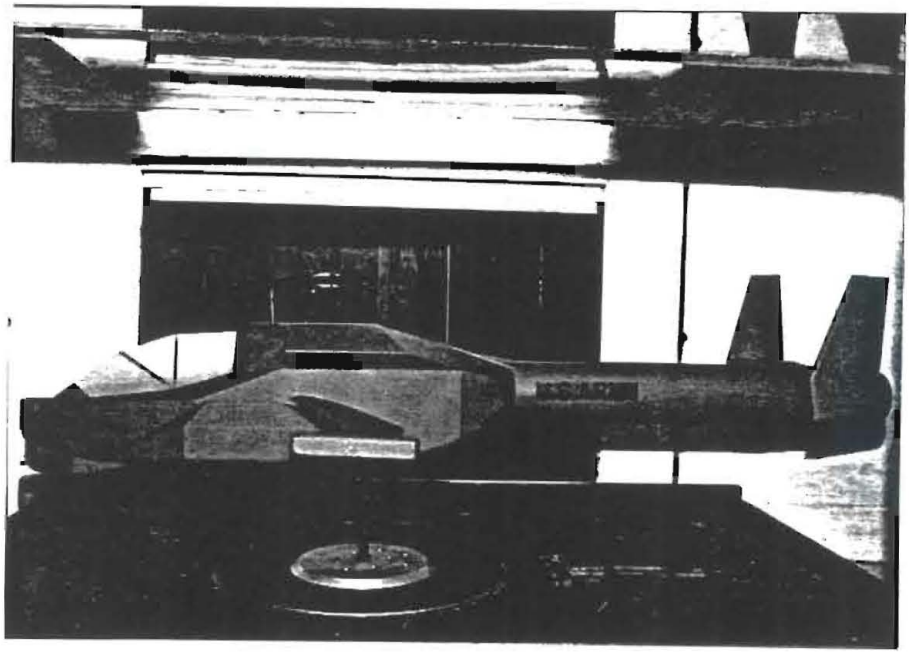

Figure 4.8 Model with Rotor Hub

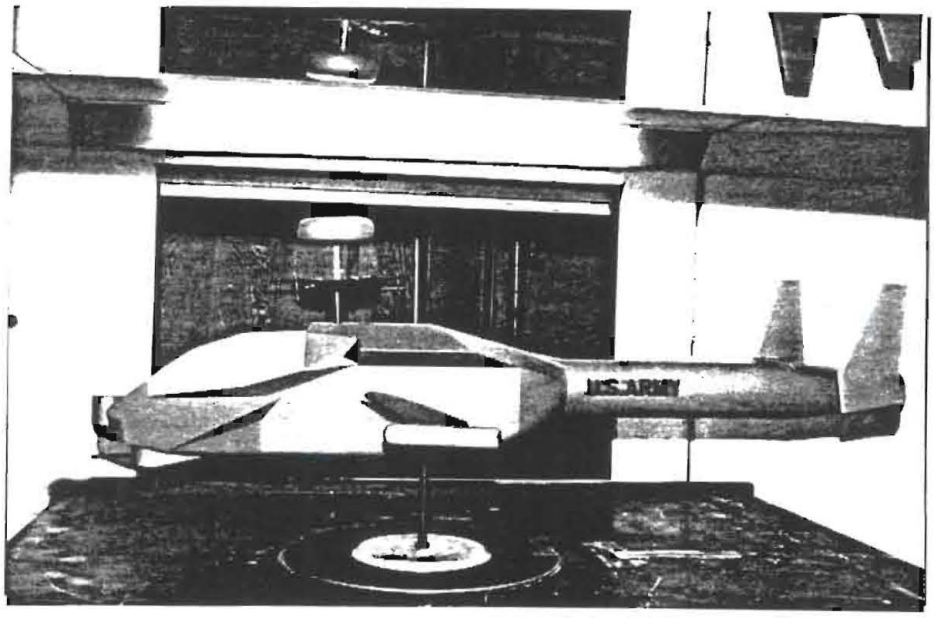

Figure 4.9 Model with Rotor Hub and Longbow Radome

Appendix A. The drag and equivalent flat plate area plots are shown in Figures 4.10 and 4.11. The average equivalent flat plate area with the rotor hub was 0.3147 ft^2. The average equivalent flat plate area with the rotor hub and the Longbow radome was 0.32467 ft^2.

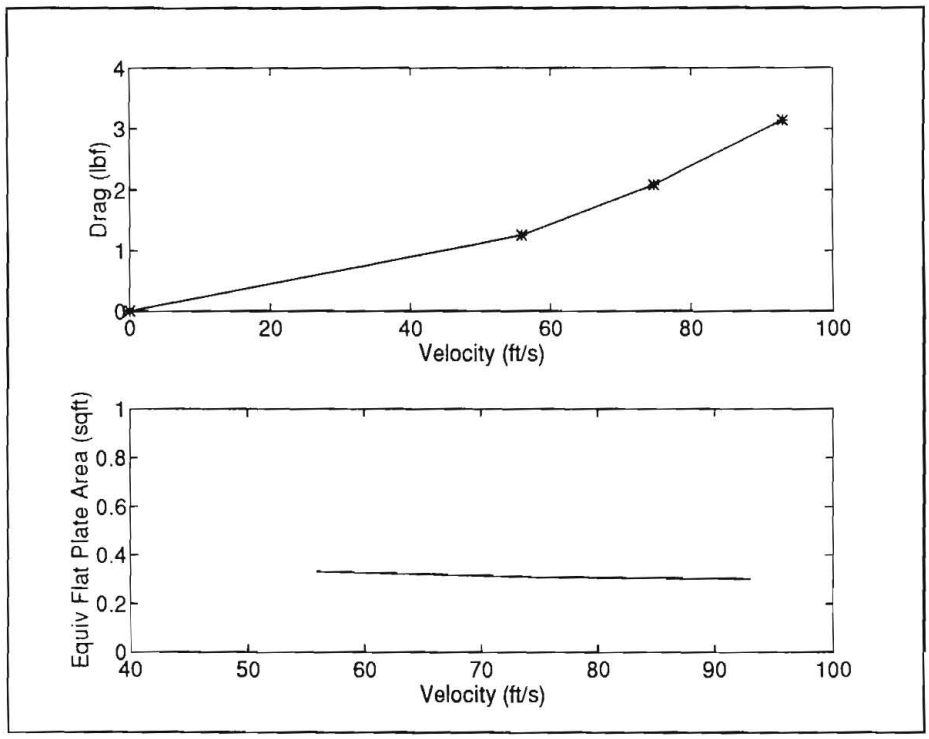

Figure 4.10 Drag and Equivalent Flat Plate Area, Model with Rotor Hub

d. Model at Varying Yaw Angles

The last run was to determine the changes in drag due to various yaw angles. The model was configured with both the rotor hub and the radome installed. Yaw angles were varied, from 10 degrees left (-10 degrees) to 10 degrees right (10 degrees) at each of three velocities, using the chain driven turntable. Data was collected at velocities of 57.2 ft/sec (33.9 knots), 71.7 ft/sec (42.4 knots), and 93.1 ft/sec (55.1 knots) and is shown in

Table A.6 in Appendix A. The drag and equivalent flat plate area at 55.1 knots were plotted versus yaw angle, and are shown in Figure 4.12.

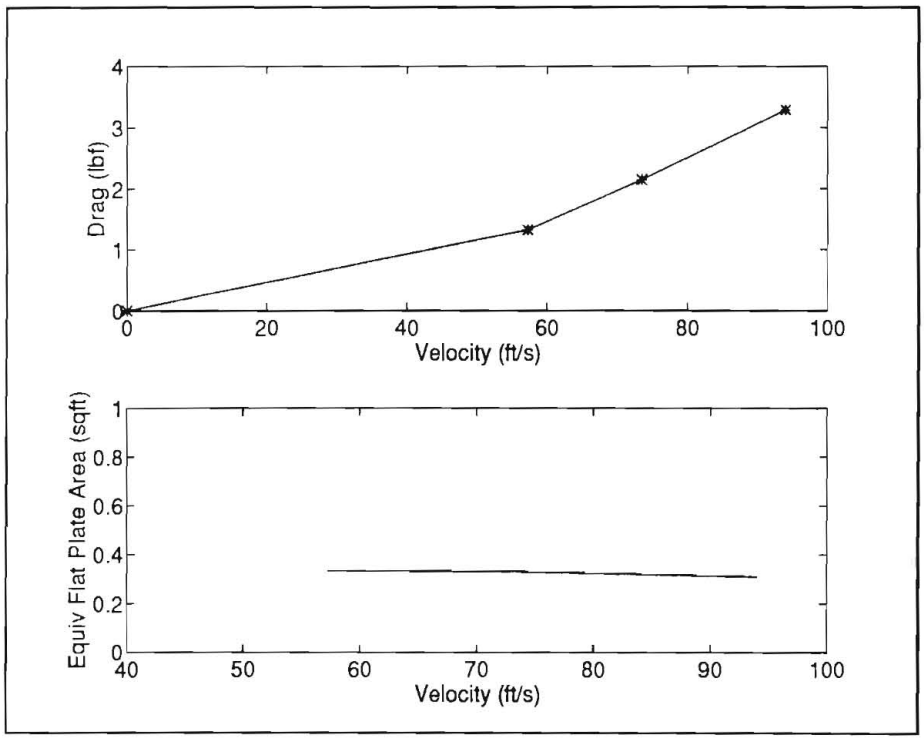

Figure 4.11 Drag and Equivalent Flat Plate Area, Model with Radome

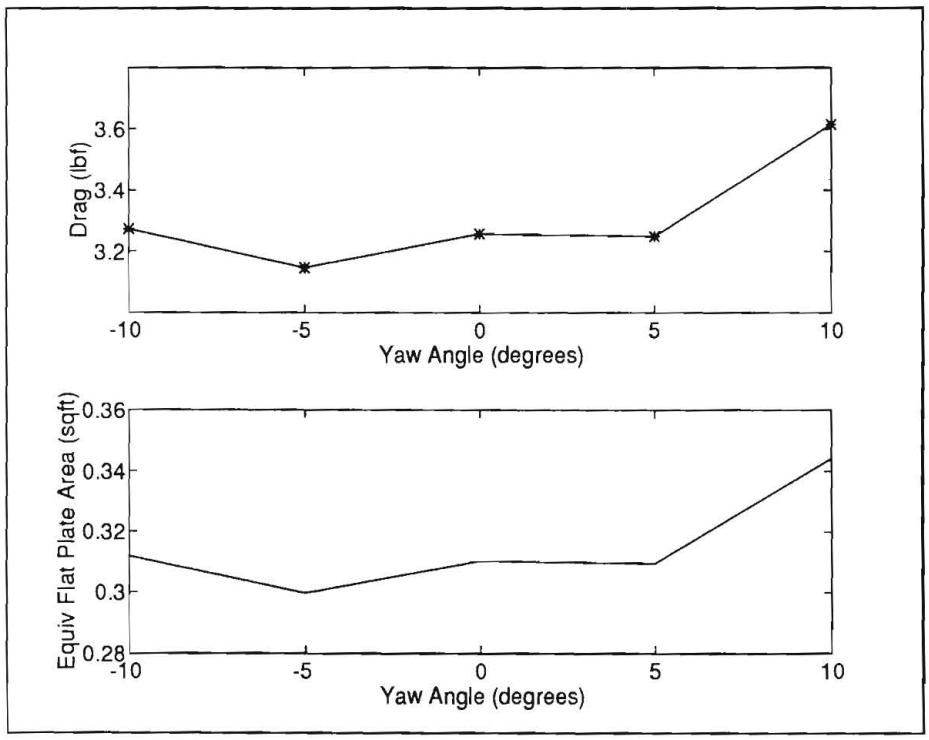

Figure 4.12 Drag and Equivalent Flat Plate Area vs. Yaw Angle

V. ANALYSIS

The data collected during the wind tunnel tests was processed to provide drag force values versus a small range of airspeeds, and in turn, the equivalent flat plate area of the Arapaho 1/12th scale model in several configurations. The purpose was to determine the validity of the wind tunnel tests by comparing the wind tunnel results to estimated values, analyze the drag on the Arapaho in the different configurations, and to compare the drag properties of the Arapaho against other modern helicopters.

A. COMPARISON OF WIND TUNNEL RESULTS TO ESTIMATED DATA

Table 5.1 shows a comparison of the estimated equivalent flat plate area of the full scale Arapaho, the estimated equivalent flat plate area of the model scaled to full size, and the measured equivalent flat plate area of the model scaled to full size.

	Model Estimate	**Full Scale Estimate**	**Model Measured**
Total	27.53 ft^2	26.50 ft^2	29.268 ft^2
w\Rotor Hub	35.13 ft^2	34.10 ft^2	41.14 ft^2
w\Hub and Radome	39.22 ft^2	38.19 ft^2	42.576 ft^2

Table 5.1 Equivalent Flat Plate Area Comparison

The measured data for the total drag on the basic fuselage was approximately 10% greater than the estimated value. The difference increases to 20% in the case of the model with the rotor hub installed, and is approximately 11% with both the rotor hub and the Longbow radome mounted on the model. It was expected that the drag on the wind

tunnel model would be higher than the estimated values because of its lower Reynolds numbers [Ref. 1, p. 291]. It is possible to extrapolate the drag on the wind tunnel model to full scale, if the amount of laminar boundary layer is known, using Figure 7.5 from Pope and Harper [Ref. 5, p. 386]. However, it is unlikely to get any more accurate. It is more practical to use the wind tunnel to approximate changes in drag due to changes in configuration [Ref. 1, p.292].

B. COMPARISON OF VARIOUS CONFIGURATIONS

The equivalent flat plate area was determined for various configurations of the model. Test runs were conducted on just the basic fuselage, the fuselage with rotor hub, the fuselage with rotor hub and Longbow radome, and the fuselage with rotor hub and radome at various yaw angles. Figure 5.1 shows a comparison of the equivalent flat plate area of the model at various airspeeds and in the three different configurations. As expected, the equivalent flat plate area increased with addition of each component of the model. There was a larger increase in equivalent flat plate area with the addition of the rotor hub than expected. This measured increase may be due in part to the lower speed and lower Reynolds number experienced at the model hub than on a full scale model. The model Longbow radome, however, produced lower drag than expected. This cannot be easily explained without further wind tunnel study.

Figure 4.12 shows the variation of equivalent flat plate area of the model at approximately 55 knots at yaw angles between 10 degrees left and 10 degrees right. Surprisingly, the plot shows a lower drag at 5 degrees left yaw than at 0 degrees (balanced

flight). This is due to the decrease in drag on the vertical tail at that yaw angle, since the vertical tail is preset at 4 degrees AOA to provide an antitorque force in forward flight.

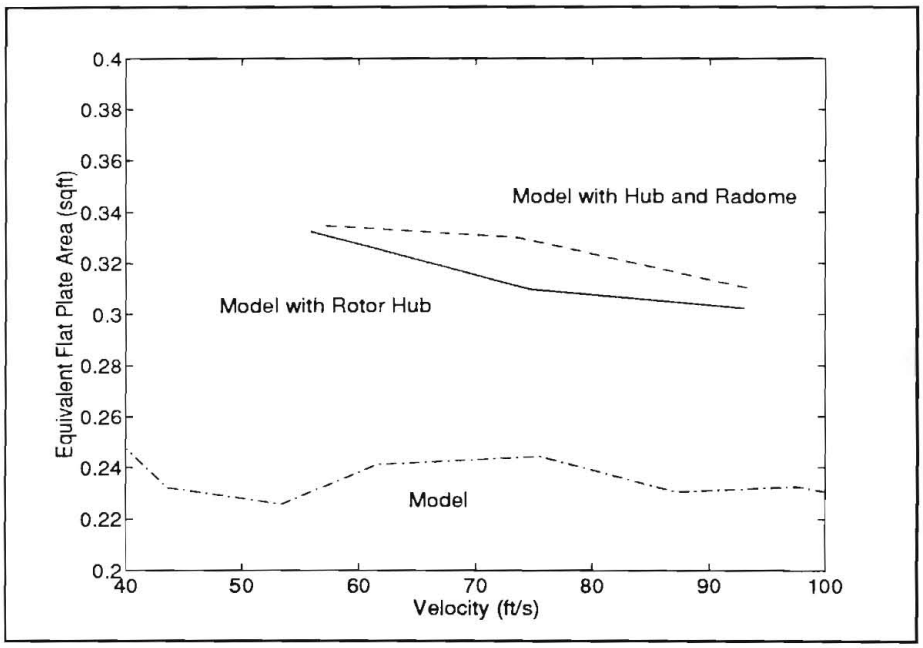

Figure 5.1 Equivalent Flat Plate Area - Different Configurations

C. COMPARISON TO OTHER HELICOPTERS

From these drag measurement values, a comparison can be made with other full scale helicopters. Table 5.2 shows a comparison of some helicopter equivalent flat plate areas.

Helicopter	$f(ft^2)$
OH6A	5.00
UH-1B	14.50
CH-47	43.20
AH-64	37.51
Arapaho Model	41.14
Arapaho Estimate	34.10

Table 5.2 Helicopter Comparison [After Ref. 1, p. 305]

In direct comparison to the AH-64 Apache, the Arapaho shows similar drag characteristics. Using information received from Mr. Harry Taylor, of McDonnell Douglas Helicopters, Table 5.3 shows an equivalent flat plate area comparison of the Arapaho against the Apache with the Longbow radome. The two aircraft are a close match.

	Arapaho Model	Apache
With Longbow Radome	42.58 ft^2	41.60 ft^2

Table 5.3 Arapaho vs. Apache

VI. CONCLUSIONS AND RECOMMENDATIONS

The Naval Postgraduate School Low Speed Wind Tunnel provided the means to do this preliminary study of the drag characteristics of a student helicopter design. This type of testing is valuable to provide quantitative feedback on student design efforts.

To obtain true full-scale drag characteristics of a helicopter, it would be best to measure it on a full scale model or aircraft installed in a full-scale wind tunnel, such as the NASA Ames 40'x80' facility at Moffet Field, California. However, this thesis has shown that the drag data obtained through the use of the 1/12 scale helicopter model, designed by students and built here at the Naval Postgraduate School, provided a reasonable approximation to a full scale aircraft design. The measured data, extrapolated to full scale, was within 10% of estimated values. While size of the model limited the effect of Reynolds Number on the drag, separation of flow could not be properly accounted for. This means the drag results of the model are somewhat higher than would have been found on the full scale aircraft.

When compared to other helicopters, the Arapaho was found by NPS wind tunnel tests to have similar drag characteristics to the Apache attack helicopter. The theoretically calculated equivalent flat plate area of the Arapaho (f=38.19 ft^2), including rotor hub and Longbow radome, was slightly less than that of the Apache (f=41.60 ft^2). While the wind tunnel measured equivalent flat plate area of the Arapaho model (f=42.58 ft^2) was slightly greater than that of the Apache. It appears that while the Arapaho design was able to reduce drag by stowing the weapons in internal bays, it may have lost some of that advantage because of the faceted shape of the nose of the fuselage. One recommendation is to test the effects of the faceted shape by doing

a wind tunnel comparison of the drag of the model with the facets, and the drag of the model with the nose of the fuselage smoothed out to a more streamlined shape.

The size of the Arapaho model was close to limits for the NPS wind tunnel. Although the cross-sectional area of the model was well within blockage limits, the model length was nearly as long as the test section. As mentioned before, this size, however, proved to be an asset regarding Reynolds number effects. In retrospect, it was clear that a balance was struck between making the model large enough to minimize scaling effects, yet keeping the model within wind tunnel limits.

Further study of the Arapaho design is recommended. Areas for wind tunnel study include a detailed study of the effects of the faceted nose section, a study of areas of flow separation, and measurements of the aerodynamic lift and moments on the model. An important area of study for both fixed and rotary wing aircraft is the trade-off between reduction in radar cross-section due to the facets and the increase in drag caused by the faceted nose.

APPENDIX A. DATA

This appendix contains the recorded data obtained during the wind tunnel test runs.

ΔP(cm H_2O)	Eaa(mV)	Ean(mV)	Eba(mV)	Ebn(mV)
0	0.02	0.02	0.02	0.11
1	0.02	0.02	0.02	0.11
2	0.03	0.02	0.01	0.11
3	0.04	0.02	0.02	0.12
4	0.06	0.02	0.02	0.12
5	0.07	0.02	0.03	0.13
6.1	0.08	0.02	0.03	0.14
7.17	0.09	0.02	0.03	0.14
8.3	0.1	0.02	0.04	0.15
9.54	0.12	0.02	0.04	0.15

Table A.1 - Model Stand Only T=63° P_m=1.017 bar

ΔP(cm H_2O)	Eaa(mV)	Ean(mV)	Eba(mV)	Ebn(mV)
0	0.01	0.03	0.04	0.07
1	0.11	0.01	0.08	0.06
1.76	0.16	0	0.11	0.03
2.25	0.21	-0.01	0.13	0.03
2.93	0.27	-0.03	0.16	0.02
3.87	0.36	-0.03	0.21	0.02
4.49	0.41	-0.05	0.24	0.02
5.65	0.52	-0.06	0.3	0.01

Table A.2 - Model and Stand, Run 1 T=64°F P_m=1.017 bar

ΔP(cm H_2O)	Eaa(mV)	Ean(mV)	Eba(mV)	Ebn(mV)
0	0.01	0.03	0.02	0.04
0.5	0.06	0.02	0.04	0.03
1	0.09	0.02	0.05	0.03
1.5	0.13	0.01	0.07	0.02
2	0.18	0	0.09	0.01
3	0.28	-0.02	0.14	0.01
4	0.36	-0.03	0.19	0
5	0.45	-0.07	0.24	0
6	0.54	-0.08	0.29	-0.01
6.57	0.62	-0.08	0.33	-0.01
7	0.63	-0.09	0.35	-0.02
7.5	0.68	-0.09	0.37	-0.03

Table A.3 - Model and Stand, Run 2 T=63°F P_m=1.016 bar

ΔP(cm H_20)	Eaa(mV)	Ean(mV)	Eba(mV)	Ebn(mV)
0	0.01	-0.01	0.01	0.01
1.65	0.2	-0.04	0.08	-0.01
2.95	0.34	-0.07	0.15	-0.03
4.56	0.52	-0.09	0.24	-0.04

Table A.4 - Model with Rotor Head T=62°F P_m=1.017 bar

ΔP (cm H_2O)	Eaa(mV)	Ean(mV)	Eba(mV)	Ebn(mV)
0	0.01	-0.01	0.01	0.01
1.73	0.22	-0.04	0.1	-0.01
2.85	0.36	-0.06	0.17	-0.02
4.66	0.56	-0.1	0.28	-0.05

Table A.5 - Model with Rotor Head and Longbow Radar T=62°F P_m=1.017 bar

Yaw Angle (degrees)	ΔP(cm H_2O)	Eaa(mV)	Ean(mV)	Eba(mV)	Ebn(mV)
0	0	0.01	-0.01	0.01	0.02
-10	1.74	0.19	0.18	0.09	0.17
-5		0.2	0.08	0.1	0.09
0		0.22	-0.05	0.11	0
5		0.21	-0.15	0.1	-0.07
10		0.21	-0.23	0.1	-0.12
-10	2.73	0.29	0.32	0.12	0.27
-5		0.32	0.14	0.17	0.14
0		0.34	-0.06	0.18	0
5		0.33	-0.24	0.17	-0.12
10		0.32	-0.36	0.17	-0.22
-10	4.61	0.47	0.54	0.2	0.45
-5		0.53	0.25	0.26	0.24
0		0.57	-0.11	0.29	-0.01
5		0.54	-0.4	0.29	-0.22
10		0.53	-0.59	0.28	-0.36

Table A.6 - Model at Various Yaw Angles T=63° P_m=1.016 bar

APPENDIX B. MATLAB PROGRAMS

This appendix contains the Matlab computer programs used to calculate and plot the drag and equivalent flat plate area graphs.

```
% Drag Force

% 5 Aug 94


%Velocity Calculation

Tm=63;                                  % Measured Settling Chamber Temp(F)
T=Tm+460;                               % Temp Conversion F to R
R=1716;                                 % Gas constant
Pm=1.017                                % Measured Ambient Pressure (bar)
Pamb=Pm*14.7*144;                       % Ambient Pressure (lbf/sqft)
Rho=Pamb/(R*T);                         % Air Density

p=[0 1 1.76 2.25 2.93 3.87 4.49 5.65];  % Measured Pressure Differential
                                        % (cm H2O)

pl=2.0456.*p;                           % Pressure Differential(lbf/sqft)

V=sqrt(2.*pl./(.913*Rho));              % Velocity Calibration Equation

e=.00817;                               % Blocking Correction

Vc=(1-e).*V                             % Corrected Velocity (ft/sec)


Vckts=Vc./1.69                          % Corrected Velocity (knots)


% Drag Force Calculation

% K= calibration matrix

K=[8.3714 -4.9115 1.0564 -1.6847
  -13.9980 164.5562 -22.3346 38.4260
  -.5946 1.7055 9.9066 -5.5392
  10.466 -36.3139 -50.1701 169.2285];

% strain gage readings

Eaa=[0 .10 .15 .20 .26 .35 .40 .51];

Ean=[0 -.02 -.03 -.04 -.06 -.06 -.08 -.09];

Eba=[0 .04 .07 .09 .12 .17 .20 .26];

Ebn=[0 -.01 -.02 -.02 -.03 -.03 -.03 -.04];

E=[Eaa; Eba; Ean; Ebn];

Drag=K(1,:)*E                           % Drag Force (lbf)

% Drag plot

subplot(2,1,1)
plot(Vc,Drag,'-',Vc,Drag,'*')
title('Drag Force - Model and Stand')
ylabel('Drag (lbf)')
xlabel('Velocity (ft/s)')



f=Drag./(.5*Rho.*Vc.^2)                 % Equivalent Flat Plat Area

% Area plot

subplot(2,1,2)
plot(Vc,f)
axis([40 120 0 1])
title('Equivalent Flat Plate Area')
ylabel('Area (sqft)')
```



```
xlabel('Velocity (ft/s)')
%axis('auto')
```

```
% Drag Force

% 5 Aug 94


%Velocity Calculation

Tm=63;                                  % Measured Settling Chamber Temp(F)
T=Tm+460;                               % Temp Conversion F to R
R=1716;                                 % Gas constant
Pm=1.016                                % Measured Ambient Pressure (bar)
Pamb=Pm*14.7*144;                       % Ambient Pressure (lbf/sqft)
Rho=Pamb/(R*T);                         % Air Density

p=[0 .5 1 1.5 2 3 4 5 6 6.57 7 7.5];    % Measured Pressure Differential
                                        % (cm H2O)

pl=2.0456.*p;                           % Pressure Differential(lbf/sqft)

V=sqrt(2.*pl./(.913*Rho));              % Velocity Calibration Equation

e=.00817;                               % Blocking Correction

Vc=(1+e).*V                             % Corrected Velocity (ft/sec)


Vckts=Vc./1.69                          % Corrected Velocity (knots)


% Drag Force Calculation

% K= calibration matrix

K=[8.3714 -4.9115 1.0564 -1.6847
  -13.9980 164.5562 -22.3346 38.4260
  -.5846 1.7055 9.9066 -5.5392
  10.466 -36.3139 -50.1701 169.2285];

% strain gage readings

Eaa=[0 .05 .08 .12 .17 .27 .35 .45 .53 .61 .62 .67];

Ean=[0 -.01 -.01 -.02 -.03 -.05 -.06 -.10 -.11 -.11 -.12 -.12];

Eba=[0 .02 .03 .05 .07 .12 .17 .22 .27 .31 .33 .35];

Ebn=[0 -.01 -.01 -.02 -.03 -.03 -.04 -.04 -.05 -.05 -.06 -.07];

E=[Eaa; Eba; Ean; Ebn];

Drag=K(1,:)*E                           % Drag Force (lbf)

% Drag plot

subplot(2,1,1)
plot(Vc,Drag,'-',Vc,Drag,'*')
title('Drag Force - Model and Stand')
ylabel('Drag (lbf)')
xlabel('Velocity (ft/s)')



f=Drag./(.5*Rho.*Vc.^2)                 % Equivalent Flat Plat Area

% Area plot

subplot(2,1,2)
plot(Vc,f)
axis([40 120 0 1])
title('Equivalent Flat Plate Area')
ylabel('Area (sqft)')
```



```
xlabel('Velocity (ft/s)')
%axis('auto')
```

```
% Drag Force Model with Rotor Head- Run 4

%23 Aug 94


%Velocity Calculation

Tm=62;                                  % Measured Settling Chamber Temp(F)
T=Tm+460;                               % Temp Conversion F to R
R=1716;                                 % Gas constant
Pm=1.017;                               % Measured Ambient Pressure (bar)
Pamb=Pm*14.7*144;                       % Ambient Pressure (lbf/sqft)
Rho=Pamb/(R*T);                         % Air Density

p=[0 1.65 2.95 4.56];

pl=2.0456.*p;                           % Pressure Differential(lbf/sqft)

V=sqrt(2.*pl./(.913*Rho));              % Velocity Calibration Equation

e=.00817;                               % Blocking Correction

Vc=(1+e).*V                             % Corrected Velocity (ft/sec)


Vckts=Vc./1.69                          % Corrected Velocity (knots)


% Drag Force Calculation

% K= calibration matrix

K=[8.3714 -4.9115 1.0564 -1.6847
  -13.9980 164.5562 -22.3346 38.4260
  -.5946 1.7055 9.9066 -5.5392
  10.466 -36.3139 -50.1701 169.2285];

% strain gage readings

Eaa=[0 .19 .33 .51];

Ean=[0 -.03 -.06 -.08];

Eba=[0 .07 .14 .23];

Ebn=[0 -.02 -.04 -.05];

E=[Eaa; Eba; Ean; Ebn];


Drag=K(1,:)*E                           % Drag Force (lbf)

% Drag plot

subplot(2,1,1)
plot(Vc,Drag,'-',Vc,Drag,'*')
title('Drag Force - Model with Rotor Hub')
ylabel('Drag (lbf)')
xlabel('Velocity (ft/s)')

f=Drag./(.5*Rho.*Vc.^2)                 % Equivalent Flat Plat Area

% Area plot

subplot(2,1,2)
plot(Vc,f)
axis([40 120 0 1])
title('Equivalent Flat Plate Area')
ylabel('Area (sqft)')
xlabel('Velocity (ft/s)')
```

```
% Drag Force Model with Rotor Head and Longbow- Run 6

%23 Aug 94


%Velocity Calculation

Tm=62;                                  % Measured Settling Chamber Temp(F)
T=Tm+460;                               % Temp Conversion F to R
R=1716;                                 % Gas constant
Pm=1.017;                               % Measured Ambient Pressure (bar)
Pamb=Pm*14.7*144;                       % Ambient Pressure (lbf/sqft)
Rho=Pamb/(R*T);                         % Air Density

p=[0 1.73 2.85 4.66];

pl=2.0456.*p;                           % Pressure Differential(lbf/sqft)

V=sqrt(2.*pl./(.913*Rho));              % Velocity Calibration Equation

e=.00817;                               % Blocking Correction

Vc=(1+e).*V                             % Corrected Velocity (ft/sec)


Vckts=Vc./1.69                          % Corrected Velocity (knots)


% Drag Force Calculation

% K= calibration matrix

K=[8.3714 -4.9115 1.0564 -1.6847
  -13.9980 164.5562 -22.3346 38.4260
  -.5946 1.7055 9.9066 -5.5392
  10.466 -36.3139 -50.1701 169.2285];

% strain gage readings

Eaa=[0 .21 .35 .55];

Ean=[0 -.03 -.05 -.09];

Eba=[0 .09 .16 .27];

Ebn=[0 -.02 -.03 -.06];

E=[Eaa; Eba; Ean; Ebn];

Drag=K(1,:)*E                           % Drag Force (lbf)

% Drag plot

subplot(2,1,1)
plot(Vc,Drag,'-',Vc,Drag,'*')
title('Drag Force - Model with Rotor Hub and Radome')
ylabel('Drag (lbf)')
xlabel('Velocity (ft/s)')

f=Drag./(.5*Rho.*Vc.^2)                 % Equivalent Flat Plat Area

% Area plot

subplot(2,1,2)
plot(Vc,f)
axis([40 100 0 1])
title('Equivalent Flat Plate Area')
ylabel('Area (sqft)')
xlabel('Velocity (ft/s)')
```

```
% Drag Force of Yawed Model with Rotor Head and Longbow- Run 6

%23 Aug 94

%Velocity Calculation

Tm=62;
T=Tm+460;
R=1716;
Pm=1.017;
Pamb=Pm*14.7*144;
Rho=Pamb/(R*T);

p=4.61;

pl=2.0456.*p;                          % Pressure Differential(lbf/sqft)

V=sqrt(2.*pl./(.913*Rho));             % Velocity Calibration Equation

e=.00817;                              % Blocking Correction

Vc=(1-e).*V                            % Corrected Velocity (ft/sec)

Vckts=Vc./1.69                         % Corrected Velocity (knots)

% Drag Force Calculation

% K= calibration matrix

K=[8.3714 -4.9115 1.0564 -1.6847
  -13.9980 164.5562 -22.3346 38.4260
  -.5946 1.7055 9.9066 -5.5392
  10.466 -36.3139 -50.1701 169.2285];

% strain gage readings

Eaa=[.46 .52 .56 .53 .52];

Ean=[.55 .26 -.10 -.39 -.58];

Eba=[.19 .25 .28 .28 .27];

Ebn=[.43 .22 -.03 -.24 -.38];

E=[Eaa; Eba; Ean; Ebn];

Yaw=[-10 -5 0 5 10];
Yawr=(pi/180).*Yaw

Ys=sin(Yawr);
Yc=cos(Yawr);
Drag1=K(1,:)*E;
Drag2=K(3,:)*E;


Drag1c=Yc.*Drag1;
Drag2c=Ys.*Drag2;

Drag=Drag1c-Drag2c

% Drag plot

subplot(2,1,1)
plot(Yaw,Drag,'-',Yaw,Drag,'*')
title('Drag Force vs Yaw Angle')
ylabel('Drag (lbf)')
xlabel('Yaw Angle (degrees)')

% Equivalent Flat Plat Area
```



```
f=Drag./(.5*Rho*Vc^2)

% Area plot

subplot(2,1,2)
plot(Yaw,f)
title('Equivalent Flat Plate Area')
ylabel('Area (sqft)')
xlabel('Yaw Angle (degrees)')
```

```
% Combined Drag Plot


% Model

%Velocity Calculation

Tm=63;                                  % Measured Settling Chamber Temp(F)
T=Tm+460;                               % Temp Conversion F to R
R=1716;                                 % Gas constant
Pm=1.016;                               % Measured Ambient Pressure (bar)
Pamb=Pm*14.7*144;                       % Ambient Pressure (lbf/sqft)
Rho=Pamb/(R*T);                         % Air Density

p=[0 .5 1 1.5 2 3 4 5 6 6.57 7 7.5];    % Measured Pressure Differential
                                        % (cm H2O)

pl=2.0456.*p;                           % Pressure Differential(lbf/sqft)

V=sqrt(2.*pl./(.913*Rho));              % Velocity Calibration Equation

e=.00817;                               % Blocking Correction

Vc=(1+e).*V                             % Corrected Velocity (ft/sec)


Vckts=Vc./1.69                          % Corrected Velocity (knots)


% Drag Force Calculation

% K= calibration matrix

K=[8.3714 -4.9115 1.0564 -1.6847
  -13.9980 164.5562 -22.3346 38.4260
  -.5946 1.7055 9.9066 -5.5392
  10.466 -36.3139 -50.1701 169.2285];

% strain gage readings

Eaa=[0 .05 .08 .12 .17 .27 .35 .45 .53 .61 .62 .67];

Ean=[0 -.01 -.01 -.02 -.03 -.05 -.06 -.10 -.11 -.11 -.12 -.12];

Eba=[0 .02 .03 .05 .07 .12 .17 .22 .27 .31 .33 .35];

Ebn=[0 -.01 -.01 -.02 -.03 -.03 -.04 -.04 -.05 -.05 -.06 -.07];

E=[Eaa; Eba; Ean; Ebn];

Drag=K(1,:)*E                           % Drag Force (lbf)


f=Drag./(.5*Rho.*Vc.^2)                 % Equivalent Flat Plat Area

%  with Rotor Head- Run 4


%Velocity Calculation

Tmh=62;                                 % Measured Settling Chamber Temp(F)
Th=Tmh+460;                             % Temp Conversion F to R
R=1716;                                 % Gas constant
Pmh=1.017;                              % Measured Ambient Pressure (bar)
Pambh=Pmh*14.7*144;                     % Ambient Pressure (lbf/sqft)
Rhoh=Pambh/(R*Th);                              % Air Density

ph=[0 1.65 2.95 4.56];
```



```
plh=2.0456.*ph;                         % Pressure Differential(lbf/sqft)

Vh=sqrt(2.*plh./(.913*Rhoh));           % Velocity Calibration Equation

e=.00817;                               % Blocking Correction

Vch=(1+e).*Vh                           % Corrected Velocity (ft/sec)

Vcktsh=Vch./1.69                        % Corrected Velocity (knots)


% strain gage readings

Eaah=[0 .19 .33 .51];

Eanh=[0 -.03 -.06 -.08];

Ebah=[0 .07 .14 .23];

Ebnh=[0 -.02 -.04 -.05];

Eh=[Eaah; Ebah; Eanh; Ebnh];

Dragh=K(1,:)*Eh                         % Drag Force (lbf)

fh=Dragh./(.5*Rhoh.*Vch.^2)             % Equivalent Flat Plat Area

% Model with Rotor Hub and Radome


Tmr=62;                                 % Measured Settling Chamber Temp(F)
Tr=Tmr+460;                             % Temp Conversion F to R
R=1716;                                 % Gas constant
Pmr=1.017;                              % Measured Ambient Pressure (bar)
Pambr=Pmr*14.7*144;                     % Ambient Pressure (lbf/sqft)
Rhor=Pambr/(R*Tr);                      % Air Density

pr=[0 1.73 2.85 4.66];

plr=2.0456.*pr;                         % Pressure Differential(lbf/sqft)

Vr=sqrt(2.*plr./(.913*Rhor));           % Velocity Calibration Equation

e=.00817;                               % Blocking Correction

Vcr=(1+e).*Vr                           % Corrected Velocity (ft/sec)

Vcktsr=Vcr./1.69                        % Corrected Velocity (knots)

% strain gage readings

Eaar=[0 .21 .35 .55];

Eanr=[0 -.03 -.05 -.09];

Ebar=[0 .09 .16 .27];

Ebnr=[0 -.02 -.03 -.06];

Er=[Eaar; Ebar; Eanr; Ebnr];

Dragr=K(1,:)*Er                         % Drag Force (lbf% Drag plot

fr=Dragr./(.5*Rhor.*Vcr.^2)             % Equivalent Flat Plat Area

% Drag plot

%subplot(2,1,1)
%plot(Vch,Dragh,'-')
```

```
%hold
%plot(Vc,Drag,'-.')
%plot(Vcr,Dragr,'--')
%title('Drag Force Comparison')
%ylabel('Drag (lbf)')
%xlabel('Velocity (ft/s)')


% Area plot

%subplot(2,1,2)
plot(Vch,fh,'-')
hold
plot(Vc,f,'-.')
plot(Vcr,fr,'--')
axis([40 100 .2 .4])
title('Equivalent Flat Plate Area')
ylabel('Area (sqft)')
xlabel('Velocity (ft/s)')
```

```
Wind Tunnel Calculated Data File

Run #1 Model Stand Only

Corrected Velocity (ft/sec)

Vc = 0 43.5745 61.6237 75.4733 87.1491 97.4356 107.6212 116.6789 125.5370 134.5882

Corrected Velocity (kts)

Vckts = 0 25.7838 36.4637 44.6588 51.5675 57.6542 63.6812 69.0408 74.2823 79.6380

Axial Drag Force (lbf)

Drag = 0 0 0.1328 0.1506 0.3180 0.3358 0.4026 0.4863 0.5041 0.6715

Equivalent Flat Plate Area (sqft)

f = NaN 0 0.0292 0.0220 0.0349 0.0295 0.0290 0.0298 0.0267 0.0309
\\\\\\\\\\\\\\\\\\\\\\\\\\\\\\\\\\\\\\\\\\\\\\\\\\\\\\\\\\\\\\\\\\\\\\\\\\\\\\\\\\\\\\\\\\\\\\\\\\\\\\\\\\\\

Run #2 Model and Stand

Corrected Velocity (ft/sec)

Vc = 0   43.5745   57.8082   65.3618   74.5876   85.7212   92.3328   103.5755

Corrected Velocity (kts)

Vckts = 0   25.7838   34.2060   38.6756   44.1347   50.7226   54.6348   61.2873

Axial Drag Force (lbf)

Drag = 0    0.6364    0.9139    1.2237    1.5743    2.0822    2.3323    2.9647

Equivalent Flat Plate Area (sqft)

f = NaN    0.2795    0.2280    0.2388    0.2359    0.2363    0.2281    0.2304
\\\\\\\\\\\\\\\\\\\\\\\\\\\\\\\\\\\\\\\\\\\\\\\\\\\\\\\\\\\\\\\\\\\\\\\\\\\\\\\\\\\\\\\\\\\\\\\\\\\\\\\\\\\

Run #3 Model and Stand

Corrected Velocity (ft/sec)

Vc = 0 30.8270 43.5960 53.3940 61.6540 75.5105 87.1920 97.4836 106.7879 111.7453 115.3441 119.3925

Corrected Velocity (kts)

Vckts = 0 18.2408 25.7964 31.5941 36.4817 44.6807 51.5929 57.6826 63.1881 66.1215 68.2510 70.6465

Axial Drag Force (lbf)

Drag = 0 0.3266 0.5287 0.7716 1.0982 1.6686 2.0990 2.6483 3.0788 3.5520 3.5438 3.8810

Equivalent Flat Plate Area from Run #3 (sqft)

f = NaN 0.2869 0.2321 0.2259 0.2411 0.2442 0.2304 0.2326 0.2253 0.2374 0.2223 0.2272
\\\\\\\\\\\\\\\\\\\\\\\\\\\\\\\\\\\\\\\\\\\\\\\\\\\\\\\\\\\\\\\\\\\\\\\\\\\\\\\\\\\\\\\\\\\\\\\\\\\\\\\\\\\
```

```
Run #4 Model with Rotor Head

Corrected Velocity (ft/sec)
Vc = 0   55.9190   74.7701   92.9608

Corrected Velocity (kts)
Vckts = 0   33.0882   44.2427   55.0064

Axial Drag Force (lbf)
Drag =  0   1.2488   2.0790   3.1395

Equivalent Flat Plate Area (sqft)
f = NaN   0.3323   0.3095   0.3023
\\\\\\\\\\\\\\\\\\\\\\\\\\\\\\\\\\\\\\\\\\\\\\\\\\\\\\\\\\\\\\\\\\\\\\\\\\\\\\\\\\\\\\\\\\\\\\\\\\\\
Run #5 Model with Rotor Head and Longbow

Corrected Velocity (ft/sec)
Vc =  0   57.2585   73.4919   93.9745

Corrected Velocity (kts)
Vckts = 0   33.8808   43.4864   55.6062

Axial Drag Force (lbf)
Drag = 0   1.3180   2.1419   3.2842

Equivalent Flat Plate Area (sqft)
f =  NaN   0.3345   0.3300   0.3095
\\\\\\\\\\\\\\\\\\\\\\\\\\\\\\\\\\\\\\\\\\\\\\\\\\\\\\\\\\\\\\\\\\\\\\\\\\\\\\\\\\\\\\\\\\\\\\\\\\\\
Run #6 Model with Rotor Hub and Longbow Radome at Various Yaw Angles

Corrected Velocity (ft/sec)
Vc = 93.4690

Corrected Velocity (knots)
Vckts = 55.3071

Yaw Angles
Yaw = -10   -5   0   5   10

Drag Forces
Drag =  3.2734   3.1462   3.2577   3.2490   3.6141

Equiuvalent Flat Plate Area (sqft)
```

f = 0.3118 0.2997 0.3103 0.3095 0.3443

LIST OF REFERENCES

1 Prouty, R.W., *Helicopter Performance, Stability, and Control*, Robert E. Krieger Publishing Company, 1990.

2 American Helicopter Society, *1993 Student Design Competition, Request for Proposal*, McDonnell Douglas Helicopter Company, 1993.

3 Naval Postgraduate School Helicopter Design Team, *Arapaho AHX*, June 1993.

4 Pope, A., *Wind-Tunnel Testing*, Second Edition, John Wiley & Sons, Inc., 1954.

5 Pope, A. and Harper, J.J., *Low-Speed Wind Tunnel Testing*, John Wiley & Sons, Inc., 1966.

6 Fisher, D.T., *Wind Tunnel Performance Comparative Test Results of a Circular Cylinder and 50% Ellipse Tailboom for Circulation Control Antitorque Applications*, Master's Thesis, Naval Postgraduate School, Monterey, California, March 1994.

7 Miller, C.W., *Cylinder Drag Experiment - An Upgraded Laboratory*, Master's Thesis, Naval Postgraduate School, Monterey, California, December 1993.

INITIAL DISTRIBUTION LIST

		No. Copies
1	Defense Technical Information Center Cameron Station Alexandria, Va. 22304-6145	2
2	Library, Code 052 Naval Postgraduate School Monterey, Ca. 93943-5002	2
3	Professor Dan Collins, Chairman, Code AA Department of Aeronautics and Astronautics Naval Postgraduate School Monterey, Ca. 93943-5002	1
4	Professor E. Roberts Wood, Code AA/Wd Department of Aeronautics and Astronautics Naval Postgraduate School Monterey, Ca. 93943-5002	4
5	Professor S. Hebbar, Code AA/Hb Department of Aeronautics and Astronautics Naval Postgraduate School Monterey, Ca. 93943-5002	1
6	Mr. Harry Taylor McDonnell Douglas Helicopter Systems 5000 East McDowell Rd. Mesa, Az. 85205	1
7	Lt Mark Couch 928 Grandy Dr. Chesapeake, Va. 23320	1
8	Mr. Ron Ramaker Department of Aeronautics and Astronautics Naval Postgraduate School Monterey, Ca. 93943-5002	1

9	Anthony Capasso 5 Tigers Ct. Trenton, N.J. 08619	1
10	LCDR Michael Capasso PSC 477 Box 35 FPO AP 96306-2735	3

DUDLEY KNOX LIBRARY
NAVAL POSTGRADUATE SCHOOL
MONTEREY CA 93943-5101

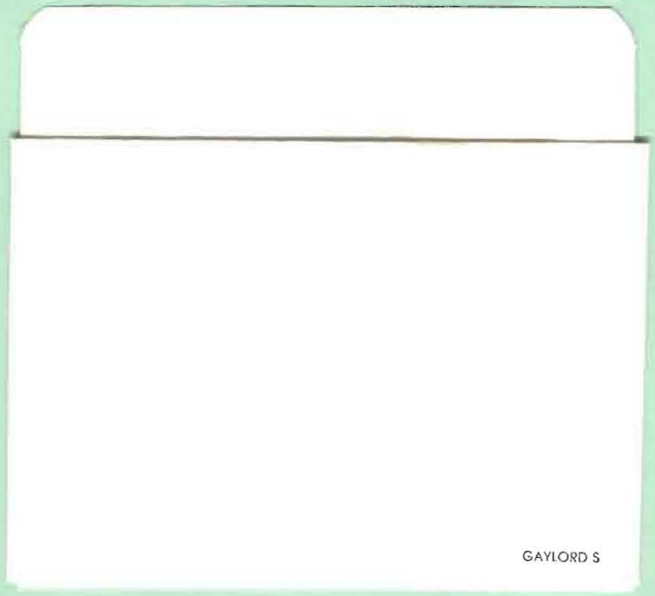

DUDLEY KNOX LIBRARY
3 2768 00302988 5